A Fundamental Adhesion Model for Asphalt

Åsa Laurell Lyne

KTH Royal Institute of Technology
School of Architecture and the Built Environment
Department of Transport Science
Division of Highway and Railway Engineering
SE-100 44 Stockholm

Doctoral Thesis

Stockholm, Sweden 2014

Preface

This doctoral thesis is based on research performed during 2009 – 2014, at the Division of Highway and Railway Engineering, Department of Transport Science, KTH Royal Institute of Technology in Stockholm, Sweden.

The main aim of this thesis was to deliver an improved understanding of the mechanism of bonding of un-aged bitumen to aggregates, with and without the addition of Portland cement, and to provide a fundamental understanding for the development of a new test method for bitumen-aggregate adhesion.

I would like to start with expressing my gratitude to my main supervisor Professor Björn Birgisson for initiating this project, providing a meaningful challenge, for his great support, valuable comments, never-ending patience and for encourage me to take a non-traditional approach in a well-researched field.

I am also sincerely grateful to Mr. Måns Collin and Docent Per Redelius for guiding me through this work and making sure that this project would have commercial relevance.

Thanks to Mr. Thorsten Nordgren at the Swedish Transport Administration for providing the bitumen samples and to Mr. Måns Collin for providing the aggregate samples.

I am thankful to Mrs. Agneta Arnius for her friendly support and to all the other staff members and PhD friends I have met through my PhD studies.

The experimental work was performed at the Division of Highway and Railway Engineering, at the Division of Surface and Corrosion Science, at the Department of Electromagnetic Engineering, and at SP Technical Research Institute of Sweden (YKI). Many thanks go to co-authors that I have had the opportunity to work with.

Lastly, but not least, I would like to thank my husband Professor Bruce Lyne for his love and support and for English correction and my children Lauren Lyne and Hallsten Lyne for understanding my preoccupation with sorting out the mysteries of asphalt adhesion.

Åsa Laurell Lyne
Stockholm, April 2014

Abstract

One of the mechanisms for the deterioration of asphalt is debonding. This is often referred to as stripping. Most losses of adhesion at the bitumen-aggregate interface are attributed to the action of water leading to a reduction in properties such as tensile strength, tensile stiffness and wear resistance. If we move to more accurate models for predicting bitumen-aggregate adhesion based on material properties, then we can be much more effective in building roads that are stable and resist hardening, crack-building, and stripping more effectively.

The main aim of this doctoral thesis was to propose a hypothesis for what makes bitumen binders stay adhered to aggregates (or filler particles such as Portland cement) and to provide a fundamental understanding for the development of a new test method for bitumen-aggregate adhesion.

The Hamaker constant was used to estimate van der Waals interactions. Hamaker's constant is composed of two parts. The first part describes the Keesom and Debye contribution, which represents the attraction energy at zero-frequency, and the second part the London dispersive (electronic) contribution, which represents the attraction energy in the optical/UV spectrum. Calculations of Hamaker's constant require accurate dielectric data, i.e. the dielectric constant and the refractive index of the interacting materials and the intervening medium.

Paper I: Hamaker's constant was introduced to describe and calculate the van der Waals interaction and to determine its relationship to resistance to stripping.

Paper II: The dispersive component of minerals was calculated from their refractive indices using data from mineral data sheets.

Paper III: The dispersive component of un-aged bitumen and aggregates was calculated from their refractive indices, determined by ellipsometery measurements.

Paper IV: The surface force mapping technique, AFM QNM, was used to measure parameters such as topography, adhesion and elastic modulus simultaneously on un-aged 70/100 penetration grade bitumen binders. The result was presented as images representing individual and overlaid parameters, e.g. topographic images with an adhesion overlay and topographic images with a modulus overlay. The adhesion forces measured in the region surrounding (peri phase) the 'bees' (catana phase) and the region in the 'bee' areas are lower than the adhesion force measured in the smooth matrix (para phase). Likewise it can be observed that Young's moduli in the region surrounding (peri phase) the 'bees' (catana phase) and in the 'bees' are higher than Young's modulus of the smooth matrix (para phase).

Paper V: The mechanism for bee formation was investigated via AFM.

Paper VI: The bitumen components that are expected to migrate to the air interface and to the surface of laboratory glass slides (or to the surface of aggregates), were investigated based on the relative dielectric spectroscopic response of the material components, as determined by their dielectric constants and refractive indices.

The total polarizability can be determined from the dielectric constant. The non-polar London dispersive (electronic) polarizability can be determined from refractive index measurements. In materials with higher permittivity at zero frequency the Keesom and Debye attraction energies will be responsible for a significant part of the polarization. Bitumen as a whole has a low degree of total polarizability. Bitumen contains a small fraction of n-heptane insoluble molecules that have a somewhat higher total polarizability and therefore may contribute to Debye and Keesom interactions. Bitumen as a whole is highly London dispersive (electronic) polarizable and the asphaltene (or n-heptane insoluble) fraction is even higher London dispersive (electronic) polarizable. The degree of non-polar London dispersion polarizability increases with increasing molecular size and with increasing aromaticity.

Paper VII: Adhesion properties of un-aged 70/100 penetration grade bitumen binders were probed by means of permittivity analysis.

The initial adhesion of non-aged bitumen binders to pure quartz aggregates is primarily London dispersive due to low total polarizability of the components.

The higher surface coverage with the addition of the Portland cement to the surface of the aggregates can be explained by the addition of components with higher London dispersive polarizability and higher total polarizability of CaO, MgO and iron oxides. Portland cement is a material contributing to Debye and Keesom interactions. Portland cement could also have chemical influence on its bonding to aggregates.

A strong correlation was identified between the average tangent of the dielectric loss angle in the frequency region of 0.01 to 1 Hz and surface coverage (a common method to indicate suitability of bitumen for use in roads). Surface coverage is higher for bitumen binders having a larger average loss tangent.

It is suggested that the average tangent of the dielectric loss angle in the frequency range of 0.01 to 1 Hz, could be used as an indicator for predicting polarizability and thereby, adhesion potential of bitumen binders.

Publications

This thesis is based on the following appended papers, referred to by their roman no.

Paper I: Lyne, Å.L., Birgisson, B., and Redelius, P. (2010). Interaction Forces Between Mineral Aggregates and Bitumen Calculated using the Hamaker Constant. *Road Materials and Pavement Design, EATA, 305-323.*

Paper II: Lyne, Å.L., Redelius, P., Collin, M., and Birgisson, B. (2013). Characterization of Stripping Properties of Stone Material in Asphalt. *Materials and Structures 46:47–61.*

Paper III: Lyne, Å.L., Krivosheeva, O., Birgisson, B. (2013). Adhesion Between Bitumen and Aggregate: Implementation of Spectroscopic Ellipsometry Characterization and Estimation of Hamaker's Constant. *Materials and Structures 46:1737–1745.*

Paper IV: Lyne, Å.L., Wallqvist, V., and Birgisson, B. (2013). Adhesive Surface Characteristics of Bitumen Binders Investigated by Atomic Force Microscopy. *Fuel 113: 248-256.*

Paper V: Lyne, Å.L., Wallqvist, V., Rutland, M., Claesson, P., and Birgisson, B. (2013). Surface Wrinkling: The Phenomenon Causing Bees in Bitumen. *Journal of Materials Science 48: 6970-6976.*

Paper VI: Lyne, Å.L., Collin, M., and Birgisson, B. (2014). Obstacles to Measuring Bitumen Surface Energy as it Pertains to Adhesion in Asphalt. *Submitted to Journal of Materials Science.*

Paper VII: Lyne, Å.L., Taylor, N., Jaeverberg, N., Edin, H. and Birgisson, B. (2014). Low Frequency Dielectric Spectroscopy of Bitumen Binders. *Submitted to Fuel.*

Contributions to the Papers

The contribution of the author of this thesis is as follows:

Paper I

The author proposed using the Hamaker model for bitumen-aggregate adhesion after taking Professor Mark Rutland's doctoral course 'Applied surface and colloid chemistry', F3B5281.
Per Redelius wrote the four first paragraphs in section 2.Theoretical background.
The author extracted the data from the literature and carried out the data analysis.
The paper was witten by the author and reviewed by the co-authors.

Paper II

The author proposed using refractive index to estimate the dispersive van der Waals' component for minerals and aggregates.
The author extracted the data from the literature and carried out the data analysis.
The paper was witten by the author and reviewed by the co-authors.

Paper III

Olga Krivosheeva performed the ellipsometer measurements on bitumen. The author conducted the refractive index measurements after being trained by Rasmus Bodvik.
Olga Krivosheeva wrote section 2.2 in the Experimental section. The rest of the paper was written by the author and then reviewed by the co-authors.

Paper IV

My thesis advisor Björn Birgisson suggested using AFM measurements on bitumen and that I take the course 'Introduction to scanning probe microscopy', F5A5677.
The author planned the experiments and prepared the samples for the AFM measurements.
Viveca Wallqvist conducted the AFM measurements and wrote section 3.2.3 in the Methods section.
The rest of the paper was written by the author and reviewed by the co-authors.

Paper V

The author planned the experiments, prepared the samples for the AFM measurements and carried out the data analysis. Professor Mark Rutland proposed the bee wrinkling model.

Viveca Wallqvist conducted the AFM measurements and wrote 'AFM force mapping' in the Methods section. The rest of the paper was written by the author and reviewed by the co-authors.

Paper VI

My thesis advisor Björn Birgisson suggested measuring surface energy of bitumen.

After having taken Professor Per Claesson's doctoral course 'Theoretical surface chemistry-surface forces', F3B5209, it became appearent that this method measures on surface films which can differ appreciably from bulk properties relevant to asphalt adhesion.

Måns Collin provided useful discussions on the mechanism for migration/exudation and further suggested the influence that extraction solvents have on perturbing the solvency parameters for a bitumen sample. He wrote the three last paragraphs on page 9. The rest of the paper was written by the author and reviewed by the co-authors.

The author and Anohe Bahramian planned the experiments and prepared the samples. Abdullah Khan conducted the sessile drop measurements. The author carried out the data analysis, and made the dielectric constant and refractive index measurements on bitumen.

Paper VII

The author prepared the samples and conducted the permittivity measurements after being trained by Nathaniel Taylor and Nadja Jaeverberg and carried out the data analysis. The paper was witten by the author and reviewed by the co-authors.

Most of the content in this thesis has been presented and discussed in Friday meetings of the Division of Highway and Railway Engineering.

Table of Contents

x

1   Introduction
1.1   Background

Many factors are known to influence moisture induced degradation of asphalt, such as aggregate and bitumen properties, processing methods, environmental factors, and traffic loading. Increased demands on life expectancy and durability of asphalt pavement has resulted in increased demand for understanding degradation processes and their dependency on the properties of bitumen, aggregates, and additives. Typical manifestations of moisture induced damage are loss of chippings, raveling, potholes, and structural damage.

Bitumen acts as a glue to hold the aggregate pavement composite together. Sufficiently strong adhesion between bitumen and aggregates is a necessity for the asphalt composite to withstand stress and moisture induced degradation. Bitumen is a complex mixture of hydrocarbons with straight or branched chains, saturated rings as well as aromatics with one up to six fused rings. The majority of the molecules are polyaromatics substituted with one or several saturated chains or saturated rings. The bitumen molecules also contain sulfur and small amounts of nitrogen and oxygen, which can be found as heteroatoms in the ring structures but also as functional groups. Traces of transition metals such as vanadium, nickel and iron may also be present depending on the source of the crude. Bitumen molecules consist of a complex combination of all these basic structures. The size of the bitumen molecules goes from about 300-400 g/mol up to about 1000-1500 g/mol. The smallest size is determined by the cut point during distillation of the asphalt. For example a cut point of 500°C corresponds to a molecular size of C35 (500 g/mol) for saturated hydrocarbons.

For a Venezuelan bitumen, the following solubility parameters were found: dispersive=18.5 MPa$^{0.5}$, polar=3.9 MPa$^{0.5}$ and hydrogen bonding=3.6 MPa$^{0.5}$ (Redelius 2006). Bitumen can interact through van der Waals forces, hydrogen bonding and pi-pi-interactions (Bagampadde 2005).

A permanent dipole is a molecule with an uneven distribution of electrons. This is typical for asymmetric molecules containing atoms with different degrees of electronegativity. In bitumen molecules the atoms which may introduce polarity are primarily nitrogen and oxygen which are considerably more electronegative than carbon and hydrogen. The total amount of nitrogen and oxygen has been determined by elemental analysis to be between 1 and 2.5 % (Jones 1993) in most bitumen used in asphalt pavements.

The surface of the aggregate is heterogeneous and varies according to mineral composition. It is also known that silica surfaces become negatively charged in neutral and basic aqueous solutions (Iler 1979). This may affect their ionic bonding potential.

This doctoral thesis incorporated the following measurements: refractive index, dielectric constant, permittivity, atomic force microscopy, and surface energy by the sessile drop method.

The main aim of this doctoral thesis was to propose a hypothesis for what makes bitumen binders stay adhered to aggregates (or filler particles such as Portland cement) and to provide a fundamental understanding for the development of a new test method for bitumen-aggregate adhesion.

Bitumen as a whole has a low degree of total polarizability. The asphaltene (or n-heptane insoluble) fraction has a somewhat higher dielectric constant than bitumen as a whole and therefore a somewhat higher degree of total polarizability. Bitumen as a whole is highly London dispersive (electronic) polarizable and the asphaltene (or n-heptane insoluble) fraction is even higher London dispersive (electronic) polarizable. The degree of non-polar London dispersion polarizability increases with increasing molecular size and with increasing aromaticity.

The higher surface coverage with the addition of the Portland cement on the surface of the aggregates can be explained by higher London dispersive polarizability and higher total polarizability of CaO, MgO and iron oxides. Portland cement can chemically bond to aggregates.

It is suggested that the average tangent of the dielectric loss angle in the frequency range of 0.01 to 1 Hz, could be used as an indicator for predicting polarizability and thereby, adhesion potential of bitumen binders.

1.2   Objectives and Delimitations

The overall aim of this doctoral thesis was to increase the understanding of what makes non-aged bitumen binders adhere to aggregates or filler particles (such as Portland cement) and to provide a fundamental understanding for the development of a new test method for bitumen-aggregate adhesion. Specific objectives were to:

- Evaluate to what extent Hamaker's constant according to Lifshitz theory can be used to calculate the van der Waal's interaction and its relationship to stripping *(Paper 1).*
- Investigate the variation in the dispersive component of minerals via their refractive indices using data from mineral data sheets *(Paper 2).*

- Quantify the refractive index of bitumen and aggregates and its relationship to bitumen–aggregate adhesion and bitumen-bitumen cohesion *(Paper 3).*
- Quantify topographic morphologies *(Paper 4).*
- Investigate mechanisms for bee formation *(Paper 5).*
- Identify obstacles to measuring bitumen surface energy as it pertains to adhesion in asphalt *(Paper 6).*
- Propose how to interpret bitumen-aggregate adhesion based on the dielectric spectroscopic response of individual material components, utilizing their dielectric constants and refractive indices *(Paper 6).*
- Introduce a potential indicator for predicting polarizability and thereby the adhesion potential of bitumen binders *(Paper 7).*

1.3   Scientific Contributions

To clarify the fundamentals of un-aged bitumen-aggregate adhesion, and determine how to choose asphalt components that can make adhesion more durable in the presence of water by determining

- the elemental composition of a mineral and its effect on refractive index and hence its dispersive adhesion to bitumen.
- the composition of bitumen and its effect on refractive index and hence dispersive interaction, and its effect on dielectric constant and hence polar interaction.
- the interaction between quartz and bitumen.
- the effect of Portland cement on bitumen-aggregate adhesion.

To examine the effects of phase separation and exudation on the surface energy of bitumen and clarify the mechanism of how 'bees' are formed.

To introduce a potential indicator for predicting polarizability and thereby adhesion potential of bitumen binders.

2   Research Methodologies

The first step was to acquire background information from the literature related to the objective of this thesis. A substantial number of literature reviews deal with bitumen-aggregate adhesion and describe this phenomenon (Isacsson 1976; Stuart 1990; Bagampadde et al. 2004; Hefer and Little 2005).

In the second step, Hamaker's contant was used to evaluate its potential for the estimation of the van der Waals interactions between bitumen and aggregate/mineral materials. The evaluation covers the usefulness of Hamaker's

constant as a tool for predicting the performance of the aggregates and minerals in resisting stripping.

In the third step, refractive index was used to estimate the dispersive component of adhesion of minerals to bitumen. Higher dispersive interactivity of minerals can be derived from the presence of specific elements in the mineral.

In the fourth step, ellipsometry was used to measure the refractive index of bitumen and aggregates. Refractive indices of aggregates are the average for the composite minerals, which in turn depend on the specific elemental composition of the minerals. The refractive index of bitumen binders is the average for the constituent components and depends upon the specific elements in the binder.

In the fifth step, atomic force microscopy was used to quantify topographic morphologies and investigate mechanisms for bee formation. Bees are a phenomenon caused by phase separation, where the phases have different rigidities and different thermal expansion coefficients resulting in differential shrinkage during cooling and ridging (interchanging higher and lower bands in the topographic surface).

In the sixth step, obstacles to measuring bitumen surface energy as it pertains to adhesion in asphalt were identified. If bitumen phase separates, and the measurements are performed on the surface only, these measurements will not give representative values for the surface energy of the bulk of the bitumen material that adheres to minerals and aggregates.

In the seventh step, the bitumen components that are expected to migrate to the air interface and to the surface of laboratory glass slides (or to the surface of aggregates) were predicted based on the dielectric spectroscopic response of their material components, as reflected by their dielectric constants and refractive indices.

In the eighth step, based on the dielectric spectroscopic response of material components, as reflected by their dielectric constants and refractive indices, bitumen-aggregate adhesion and bitumen-Portland cement-aggregate adhesion are discussed.

In the ninth step, the tangent of the dielectric loss angle in the frequency range of 0.01 to 1 Hz is introduced as a potential indicator of polarizability and thereby adhesion potential of bitumen binders.

3   Theoretical Models/Experimental Conditions

In this chapter a description is given of the theories and techniques used in this thesis.

3.1   Intermolecular Forces

Adhesion has been explained by physical forces giving rise to physical bonds between discrete atoms and molecules. Asphalt materials form condensed solid or liquid phases, and are held together by intermolecular van der Waals forces.

Van der Waals forces originate from the interactions between atomic or molecular rotating or oscillating dipoles within the medium. For a description of the van der Waals forces, see the books 'Intermolecular and Surface Forces' by Israelachvili (1991) and 'van der Waals forces - Interaction Forces Using the Hamaker Constant' by Parsegian (2006). Chemical bonds hold molecules together within a material by electron sharing between two or more atoms. Physical bonds are not bonds in this conventional meaning; they are attractive forces holding the material(s) together by long-range physical forces. They are always the controlling forces when no chemical bonds are established between the materials. A physical bond does not have the strong directionality of chemical bonds. This is why the molecules can rotate and still stay bonded. For liquids this may be slightly more obvious than for a glue-like material such as bitumen. However, the mechanism is the same.

It was recognized in the first half of the 1900's that van der Waals forces are the dominant electromagnetic interaction forces responsible for the stability of colloids and important in adhesion.

There are three types of van der Waals physical interaction forces (Israelachvili 1991; Parsegian 2006): dipole-dipole (Keesom or orientation forces), dipole-induced-dipole (Debye or induction forces), and induced-dipole-induced dipole interactions between two non-polar molecules (London or dispersive forces). These forces all decay with distance r to the power of r^{-7}, and the interaction energies decay with r^{-6}.

Dipole-dipole interactions (Keesom or orientation interaction): Due to shape and uneven distribution of charges within their atoms, certain molecules develop permanent dipole moments, i.e. they are polar molecules. When two of these polar molecules are near each other there is a dipole-dipole interaction between them that is similar to the alignment between two magnets. The energy of interaction between two rotating dipoles can be expressed as the Keesom or orientation interaction, see *Equation 1*:

$$w(r) = -\frac{u_1^2 u_2^2}{3(4\pi\varepsilon_0\varepsilon_r)^2 kT r^6} \qquad (1)$$

where *u* is the dipole moment, ε_0 is the permittivity of free space, ε_r is the dielectric constant of surrounding material, and *r* is the distance between molecules, *k* is the Boltzmann's constant and *T* is absolute temperature.

Dipole-induced dipole interactions (Debye or induction interaction): The interaction between a polar molecule and a non-polar molecule is due to the polarizing field that comes from a polar molecule polarizing another atom or nonpolar molecule i.e. similar to a magnet attracting a piece of iron.

The energy of interaction between a rotating dipole and an induced dipole (both molecules having a permanent dipole moment) can be expressed as the Debye dipole-induced dipole interaction, see *Equation 2*:

$$w(r) = -\frac{u_1^2 \alpha_{02} + u_2^2 \alpha_{01}}{(4\pi\varepsilon_0\varepsilon_r)^2 r^6} \qquad (2)$$

where α_0 is the London dispersive (electronic) polarizability.

Induced-dipole-induced dipole interactions / two non-polar molecules (London or dispersion interaction): The interaction between non-polar molecules is due to the random fluctuation of an atom's electronic distribution with time. The dipoles generate an electric field that polarizes any nearby neutral atom, inducing a temporary dipole moment in it. This creates an attraction between the molecules.

The energy of interaction between two different molecules with induced dipole-induced dipole, can be expressed as the non-polar London induced dipole-induced dipole interaction, see *Equation 3*:

$$w(r) = -\frac{3}{2}\frac{\alpha_{01}\alpha_{02}}{(4\pi\varepsilon_0\varepsilon_r)^2 r^6}\frac{h\nu_1\nu_2}{(\nu_1 + \nu_2)} \qquad (3)$$

where *h* is Planck´s constant and ν is the molar volume.

The magnitude of the dispersion forces increase with increasing molecular size because the electrons will be further away from the nucleus the larger the molecule is. Since increasing molecular size normally means increasing molecular mass, it could be said that the dispersion forces increase with increasing molecular mass. Dispersion forces exist between all molecules whether they are polar or not.

These types of interaction forces are present between all atoms and molecules, even between the ones that are totally neutral. Since these forces are always present (in contrast to Keesom and Debye that may or may not be present due to the properties of the molecule) they play an important role in phenomena such as adhesion, physical adsorption, surface tension, wetting, and the properties of gases, liquids and thin films.

In *Paper VI* and *Paper VII,* initial bitumen-aggregate adhesion and bitumen-Portland cement-aggregate adhesion are discussed based on the dielectric spectroscopic response of the material components, as reflected by their dielectric constants and refractive indices. It was argued that quartz aggregates and bitumen as a whole have low total polarizability and the interaction energy should be expressed as primarily induced-dipole-induced dipole interaction energy. Portland cement is however at least partly a polar material since it contains oxides with intermediate and high total polarizability.

In addition to the van der Waals forces, hydrogen bonds can be formed when a hydrogen atom in a molecule is attracted to a strongly electronegative atom in another molecule such as nitrogen, oxygen, or fluorine.

3.2 Hamaker

The Hamaker constant according to Lifshitz theory represents the Keesom, Debye and London Forces of the van der Waals attraction between two materials. The Hamaker constant is a continuum theory and can only be used when the interacting surfaces are farther apart than molecular dimensions (Israelachvili1991). The van der Waals forces arise from the interaction between dipoles and fluctuating dipoles. Hamaker constant is calculated from the dielectric constants of materials measured at zero frequency and in the optical/UV portion of the spectrum.

If the absorption frequencies of the interacting materials and intervening media are assumed to be the same, then the Hamaker constant, A, for two materials 1 and 2 interacting across a medium 3 can be calculated according to the Lifshitz theory (1956) in *Equation 4*:

$$A = A_1 + A_2 = \frac{3kT}{4}\left(\frac{\varepsilon_1-\varepsilon_3}{\varepsilon_1+\varepsilon_3}\right)\left(\frac{\varepsilon_2-\varepsilon_3}{\varepsilon_2+\varepsilon_3}\right) + \frac{3h\nu}{8\sqrt{2}}\frac{(n_1^2-n_3^2)(n_2^2-n_3^2)}{\sqrt{n_1^2+n_3^2}\sqrt{n_2^2+n_3^2}\left(\sqrt{n_1^2+n_3^2}+\sqrt{n_2^2+n_3^2}\right)} \quad (4)$$

where ε_i is the static dielectric constant for material/medium *i*, and *n* is the refractive index of the material/medium *i* in the visible region. *h* is Planck's constant (=6.6261·10-34 Js), *k* is Boltzmann constant (= 1.3807·10-23 J/K), *T* is the absolute temperature and *v* is the main electronic absorption frequency typically around 3·1015 s^{-1}.

The first term (A_1) represents the zero-frequency energy of the van der Waals interaction and includes the Keesom and Debye dipolar contributions. The second term (A_2) represents the dispersion energy and includes the London energy contribution.

For most material combinations the Hamaker constant is positive and the van der Waals force is attractive. The van der Waals force is always attractive between two like surfaces and always attractive in vacuum (air). The Hamaker's constant can be negative and repulsive for two different material surfaces interacting through a liquid medium.

If Hamaker's constant is zero, there is no net force, and the bodies are neither pulled together nor pushed apart. However, if the net force is positive, then the bodies will adhere, and if the net force is negative repulsion will occur.

Hamaker (1937) calculated the van der Waals interaction free energies between bodies of different geometries on the basis of pairwise additivity. The forces were obtained by differentiating the energies with respect to distance. For example, the van der Waals interaction *(W)* for a flat surface interacting with another flat surface can be calculated using *Equation 5*:

$$W = -\frac{A}{12\pi D^2} \qquad\qquad (5)$$

where D is the surface separation distance. A derivation of this equation is given by Israelachvili (1991). As can be seen in *Equation 5*, there is a direct relationship between the van der Waals interaction and the Hamaker constant.

In the pioneer work by Hamaker (1937), the constant was calculated from the polarizabilities and number densities of the atoms in the two bodies by postulating pair-wise additivity of the contributions from individual molecules. This pair-wise approach ignores however the many-body effects and cannot easily be extended to bodies interacting in a medium. These problems are bypassed in the Lifshitz theory (1956) where the atomic structure is disregarded and treated as a continuous medium.

The van der Waals interaction and the Hamakers's constant can be calculated from frequency dependent dielectric properties of the interacting materials and their intervening medium. For the van der Waals interaction the geometry of the bodies is also required.

3.3   Dielectric Spectroscopy

Dielectric spectroscopy is an experimental technique used to characterize molecular structures and their mobility in a dielectric material. The dielectric spectroscopic response may be expressed as a function of frequency (frequency domain spectroscopy) or as a function of time (time domain spectroscopy).

A dielectric material is a material that behaves as an electrical insulator and can be polarized by an applied field (Britannica 2014). As the dielectric material is placed in an electric field, electric charges do not move through the material as they do through a conductor. There will instead be a slight shift of charges causing dielectric polarization. Positive charges will move towards the field and negative charges will move in the reverse direction. If the dielectric material consists of weakly bonded molecules, those molecules will not only become polarized, but will also be reoriented so that their symmetry axis aligns to the field. This polarization will reduce the electric field within the material.

Permittivity is a measure of how an electric field affects and is affected by a dielectric material. Permittivity is usually not constant, as it can vary with position in the medium, the frequency of the field applied, humidity, temperature, and other parameters. The main objective in studying permittivity is to relate macroscopic properties such as the dielectric constant to microscopic properties such as the molecular polarizability and the dipole moment of the molecules. Polarizability is the relative tendency of a material to have a charge distribution (or distortion of an electron cloud of an atom or molecule from its normal shape) caused by an external electric field. Polarizability determines the response of a certain material to external fields and its susceptibility to induced polarity.

Refractive Index and Dispersive Polarizability. The refractive index of a material is a measure of the speed of light in that substance in relation to the speed of light in vacuum. For example, the refractive index of water is 1.33, meaning that light travels 1.33 times faster in a vacuum than it does in water. Thus, the refractive index, n, is expressed as *Equation 6*:

n = velocity of light in a vacuum / velocity of light in medium. (6)

According to the Lorenz–Lorentz equation, the London dispersive (electronic) polarizability, α_0, is related to the chemical structure of the material through the refractive index, n, see *Equation 7*:

$$\frac{\alpha_0}{(4\pi\varepsilon_0)} = \left(\frac{n^2-1}{n^2+2}\right)\frac{3v}{4\pi} \qquad (7)$$

where $v = \frac{M}{\rho N_0}$, M is the molecular weight, ρ is the mass density, and N_0 is Avogadro's number, and ε_0 is the permittivity of free space.

The trend of polarizability follows the size of the molecule, hence the number of electrons, thus polarizability increases with the size of molecules.

The measurements of refractive index were conducted with a phase-modulated ellipsometer (Beaglehole Instruments, Wellington, New Zealand) on the bitumen binder samples. It is an optical surface sensitive technique, which is widely used for measurements in thin surface layers (Narayanamurti et al. 1976; Naderi et al. 2007). The instrument relies on the fact that
- reflection at a dielectric interface depends on light polarization.
- the transmission of light through a layer changes the phase of the incoming wave depending on the refractive index of the material.

Refractive index also depends on the temperature, which can become relevant when polymers are heated above their transition temperatures (i.e. Tg, above which the polymer chain mobility increases).

Some minerals have more than one refractive index, and thus can have different refractive indices in different directions.

Dielectric Constant and Total Polarizability. The dielectric constant is a measure of the extent of polarization in induced and permanent dipoles. The propensity of the material to respond to an applied field therefore increases with extent of polarization in induced and permanent dipoles. The response is caused by a reorientation of microscopic dipoles. In materials with higher permittivity at zero frequency the Keesom and Debye attraction energies will be responsible for a significant part of the polarization.

The dielectric constant is also a measure of the influence a substance has on the energy that is required to separate or produce two oppositely charged bodies. Substances that can produce a hydrogen bonded network have high dipole moments and high dielectric constants (Ghosh and Jasti 2005).

According to the Clausius-Mossotti equation, the total polarizability, α, is related to the chemical structure of the material through the dielectric constant, ε_r, see *Equation 8*:

$$\frac{\alpha}{(4\pi\varepsilon_0)} = \left(\frac{\varepsilon_r-1}{\varepsilon_r+2}\right)\frac{3v}{4\pi} \qquad (8)$$

where $v = \frac{M}{\rho N_0}$, M is the molecular weight, ρ is the mass density, and N_0 is Avogadro's number, and ε_0 is the permittivity of free space.

The relative complex permittivity, ε_r, of a material is defined in *Equation 9*:

$$\varepsilon_r = \varepsilon'_r - j\varepsilon''_r \qquad (9)$$

Permittivity as a function of frequency has real, ε'_r, and imaginary, ε''_r, values, see *Equations 10 and 11*:

$$\varepsilon'_r = \frac{d \cdot C_P}{\varepsilon_0 \cdot A} \tag{10}$$

$$\varepsilon''_r = \frac{d \cdot C_S}{\varepsilon_0 \cdot A} \tag{11}$$

where C_p and C_s are the real and imaginary parts of complex capacitance measured by a frequency impedance analyzer. The real part of permittivity, ε'_r, is referred to as the dielectric constant and represents stored energy when the material is exposed to an electric field, while the imaginary part of permittivity, referred to as the dielectric loss factor, ε''_r, represents the energy that is lost in the applied field. Vacuum permittivity, ε_0, is ~8.85x10^{-12} F/m. Vacuum permittivity also appears in Coulomb's law as a part of the Coulomb force constant $\frac{1}{4\pi\varepsilon_0}$ which expresses the force between two unit charges separated by unit distance in vacuum.

The tangent of loss angle is, tan δ, defined as the ratio of the imaginary part to the real part in *Equation 12*:

$$\tan\delta = \frac{\varepsilon''_r}{\varepsilon'_r} = \frac{C_S}{C_P} \tag{12}$$

The measurements of capacitance and loss at power frequency are often presented as the real and imaginary part of the complex relative permittivity, ε_r, and is referred to as the dielectric response. For dielectric materials such as bitumen, the spectra are often measured from mHz to kHz, and sometimes up to MHz.

Under a sinusoidal field, the current density can be written as (Linhjell et al. 2007), see *Equation 13*:

$$J(\omega) = E(\omega)\, i\varepsilon_r\omega \left[1 + \chi'(\omega) - i\left(\frac{\sigma}{\varepsilon_0\omega} + \chi''(\omega)\right) \right] \tag{13}$$

where ω is the angular frequency, σ is the DC conductivity, and χ' and χ'' are the real and imaginary components of the complex susceptibility.

The real component of ε_r can be determined by *Equation 14*:

$$\varepsilon'_r = 1 + \chi'(\omega) \tag{14}$$

The imaginary component of ε_r can be determined by *Equation 15*:

$$\varepsilon''_r = \frac{\sigma}{\varepsilon_0\omega} + \chi''(\omega) \tag{15}$$

This means that the conductivity contributes more to the apparent ε''_r at low frequencies than at high frequencies (Linhjell et al. 2007).

An IDAX-300 Insulation Diagnostic Analyzer from Megger was used to measure dielectric permittivity. It is a low frequency impedance analyzer and was used in the frequency range from 0.01 Hz to 10000 Hz. The total area of the electrode on which

the current was measured was 41.8 cm^2 and the distance between the electrodes was 1 cm.

3.4 Atomic Force Microscopy

The AFM Force mapping was performed on a Bruker Multimode 8 AFM in PeakForce QNM (Quantitative Nanomechanical property Mapping) mode with a Nanoscope V controller and the software Nanoscope 8.15. The resulting force curves were evaluated using Nanoscope Analysis 1.30. The cantilever model was a ScanAsyst Air (Bruker) with a nominal spring constant of 0.4 N/m and a nominal tip radius of 2 nm. The exact spring constant was determined by the Thermal Tune method (Hutter and Bechhoefer 1993) and the tip radius was calibrated with Bruker references PDMS-SOFT-2-12M, i.e. PDM with a known DMT Young's modulus of 3.5 MPa. Force mapping was performed as follows: the sample was oscillated in the z-direction at 2 KHz at the same time as the sample was scanned line by line at a rate of 1 Hz perpendicular to the cantilever. Every image was built up by 512x512 pixels each originating from force curve evaluation.

3.5 Thermodynamic Adsorption

The thermodynamic adsorption theory relates adhesion to surface energy. When a surface is created, surface energy is used as a quantification of the disruption of intermolecular bonds. The surface energy is defined as the excess energy at the surface compared with bulk. The two-component theory and the acid-base theory are the two most common thermodynamic theories.

The Owens-Wendt model was introduced in (1967) and is based on two components, see *Equation 16*:

$$\gamma_L(1 + cos\theta) = 2(\sqrt{\gamma_L^{LW}\gamma_S^{LW}} + \sqrt{\gamma_L^{P}\gamma_S^{P}}) \qquad (16)$$

where *LW* refers to the non-polar Lifshitz-van der Waals (LW) interaction and the *P* refers to the polar interactions. The Owens-Wendt approach is one of the most common methods (Zenkiewicz 2007) for calculating the surface free energy of polymeric materials.

3.6 Surface Coverage

The rolling bottle method was used according to SS-EN 12697-11. The amount of bitumen remaining on aggregates is visually determined after mechanical stirring of bitumen-covered aggregates in water. When Portland cement was added, it was added to the aggregates that had been heated prior to bitumen being added to the mix. The samples were photographed after 24 hours and the percentage bitumen adhering to quartzite aggregates was determined after 24 hours agitation in water.

4   Results and Discussion

4.1   Interaction Forces Between Mineral Aggregates and Bitumen Calculated Using the Hamaker Constant

In this paper Hamaker's constant was introduced to describe and calculate the van der Waals interaction and to determine its relationship to resistance to stripping.

The dielectric properties of the aggregates and minerals studied were collected from different sources and are summarized in *Table 1*.

Table 1   Dielectric properties (for references see *Paper I*).

Aggregate	Dielectric constant, ε	Refractive index, n
Bitumen	2.6	n=1.58
Air	1	n=1
Water	80	n=1.33
Basalt	8	n=1.62-1.74
Granite (weathered)	5	n=1.45, 1.56 (different granites)
Calcite	7.8-8.2	n=1.49-1.66
Quartz	4.2-5	n=1.55

The Hamaker constant expresses a practical way to calculate van der Waals interaction by using the dielectric properties of two interacting bodies and the intervening medium. The minerals have been ranked according to their maximum Hamaker constant. Basalt has the highest (high) Hamaker constant and granite (hyalite) has the lowest (high) Hamaker constant (see *Table 2*).

The aim was also to calculate and determine the importance of the permanent dipolar and induced dipolar dispersive contributions to the interaction between bitumen and the different aggregates and minerals, using water or air as intervening medium. Hamaker's constant zeros-in on the induced dipole dispersive contribution of van der Waals adhesion.

Table 2   Permanent dipolar and induced dipolar dispersive contributions for minerals and aggregates with either water or air as intervening medium. A=Hamaker's constant.

Material 1	Medium 3	Material 2	A_1 ($\cdot 10^{-20}$ J) *Permanent dipolar component*	A_2 ($\cdot 10^{-20}$ J) *Induced dipolar dispersive component*	A_{total} ($\cdot 10^{-20}$ J)
Basalt	**Air**	Bitumen	0.11 1 %	11.06 99 %	11.17
Granite	**Air**	Bitumen	0.09 1 %	7.33 99 %	7.42
Basalt	**Water**	Bitumen	0.24 9 %	2.50 91 %	2.73
Granite	**Water**	Bitumen	0.26 34 %	0.77 66 %	1.03

The numbers calculated in this study are of course approximate, but give us an idea of the relative importance of the permanent dipolar and induced dipolar dispersive contributions to the van der Waals adhesion. For air as an intervening material, the permanent dipolar contribution is negligible (about one percent). For water as an intervening medium the relative contribution is higher, between 9 and 25 percent. However, the total value of Hamaker's constant is much lower with water as intervening medium. In practice, this means that if water gets in between bitumen and aggregates, a significant reduction in adhesion is expected.

In *Table 3*, Hamaker's constant has been ranked according to its maximum value (high value of refractive index for birefringent minerals). Each Hamaker's constant value has been compared with 'resistance to stripping' –performance according to Cordon (1979). The performance of the aggregates and minerals correlates well with Hamaker's constant where resistance to stripping data is available.

Table 3   Hamaker's constant, calculated by the authors based on *Equation 4* according to Israelachvili (1991) and resistance to stripping according to Cordon (1979).

	Hamakers constant A_{total} ($\cdot 10^{-20}$ J)	Resistance to stripping Cordon (1979)
Basalt	11.06	Good
Limestone *(Dolomite)*	10.33	Good
Limestone *(Calcite)*	10.07	Good
Granite *(Kaolinite)*	8.88	Fair
Quartz	8.74	Fair (quartzite)
Albite	8.56	---
Microcline	8.54	---
Granite *(* Endelite, Allophane, Hyalite)	7.33-8.42	Fair

4.2   Characterization of Stripping Properties of Stone Material in Asphalt

In this paper the refractive index of minerals was characterized using data from mineral data sheets. This study is focused on the second part of Hamaker's equation according to Lifshitz. The mineral data that has been used in this study comes from a website that contains data sheets for more than 4000 individual minerals (Web Mineral 2011).

In the literature, minerals have been classified visually according to the degree of stripping and rated according to their tendency for stripping as slight, moderate or severe, see *Figure 1*. Stuart (1990) extracted this information (for minerals) from the literature. For each mineral there is a spread in the refractive index, i.e. refractive index varies from a lowest to a highest value for each mineral.

A higher 'high' refractive index for the minerals with a slight tendency of stripping, and a lower 'high' refractive index for those minerals that were expected to perform not as well (rated as moderate or severe tendency for stripping). As can be seen in *Figure 1*, a refractive index of the mineral higher than approximately 1.6 indicates a slight tendency for stripping, i.e. a lower tendency for stripping, and a lower refractive index than approximately 1.6 indicates a moderate to severe tendency for stripping.
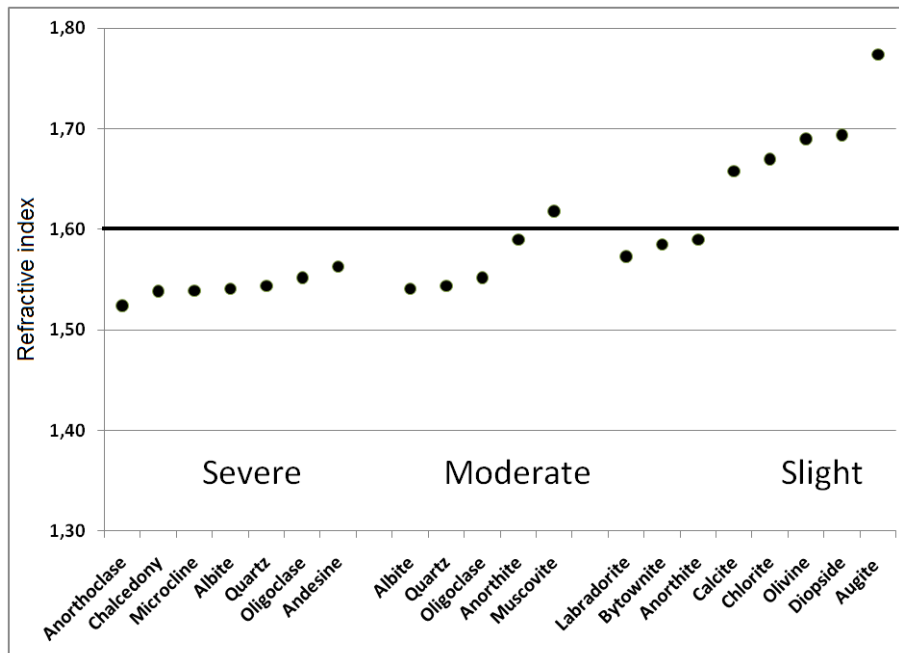

Figure 1   Minerals rated according to their tendency for stripping (Stuart 1990).

Minerals exist as more or less complicated compounds. Most of these minerals have known refractive indices. The eight most common elements of the aggregates in the Earth's crust are: oxygen, silicon, aluminum, iron, calcium, sodium, potassium,

and magnesium. In order to study the effect of elements on the refractive index of minerals, only specific minerals were selected. For each element studied, all minerals were picked that contained that specific element together with the non-metals in period one to three, i.e. H, B, C, N, O, Si, P, and S.

For example, the elements sodium, potassium and rubidium belong to the alkali metal group in the periodic table. Sodium and potassium are common throughout the earth's crust. They are all situated in group one in the periodic table.

Minerals with elements from the alkali metals group combined with elements from the non-metals group in period one to three have low refractive indices, see *Figure 2*. It can be seen in the figure that the refractive index is independent of the alkali metal content. Overall, the minerals in *Figure 2* containing alkali metals combined with n·(H, B, C, N, O, Si, P, and S) have a refractive index below approximately 1.6. According to *Equation 4*, this means that minerals containing alkali metals do not exhibit strong dispersive interactions due to their low refractive indices. Also, all alkali metals are water soluble to a degree, which increases the probability of stripping.
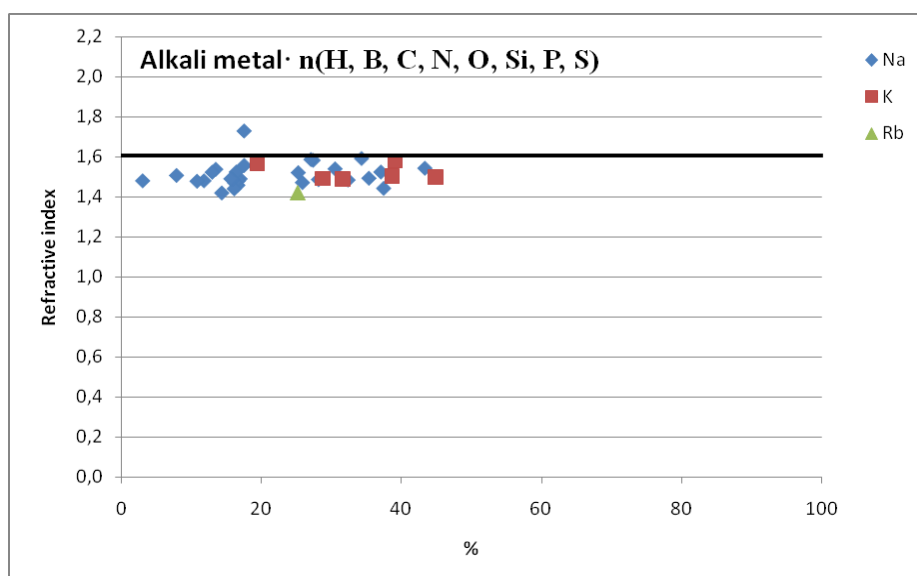

Figure 2   Refractive index, n, versus percentage of alkali metal elements in each mineral.

4.3 Adhesion Between Bitumen and Aggregate: Implementation of Spectroscopic Ellipsometry Characterization and Estimation of Hamaker's Constant

The purpose of this paper was to quantify the refractive index of bitumen and aggregates and its relationship to bitumen–aggregate adhesion and bitumen-bitumen cohesion. This study is focused on the second part of Hamaker's equation according to Lifshitz. Measurements of refractive index were performed on typical aggregates and actual bitumen binders used in asphalt pavement (see *Table 4*). The refractive indices were determined by ellipsometery measurements. Refractive index was measured on the three aggregates and seven penetration grade 70/100 bitumen binders using an ellipsometer. The aggregates studied were two types of granite and one diabase.

Each aggregate studied contains several types of minerals. For example, the main minerals of the granite from Taivassalo are: potash feldspar, quartz, plagioclase, and biotite. The main minerals of the diabase from Varpaisjärvi are: amphibole, plagioclase and pyroxene. Each mineral has its specific refractive index. Among the minerals included in the aggregates studied is pyroxene that has the highest refractive index, and feldspar potash that has the lowest refractive index. It can be noticed that there is quite a large difference in the refractive index among the different minerals.

Refractive indices of bitumen binders are the average of constituent components and will be dependent upon the specific elements in the binder.

Table 4   Refractive index for three different aggregates samples and seven bitumen samples.

SAMPLE	REFRACTIVE INDEX
Bitumen binders a to g	**1.550 – 1.595**
Diabase (V)	1.712
Granite (T) - pink	1.570
Granite (T) - black	1.542
Granite (K)	1.544

4.4 Adhesive Surface Characteristics of Bitumen Binders Investigated by Atomic Force Microscopy

In this study, microphase-separated topographic morphology was investigated by AFM QNM on unaged penetration grade 70/100 bitumen binder, and the effect on local mechanical properties has been measured. AFM QNM is a surface force mapping technique which measures parameters such as topography, adhesion and elastic modulus simultaneously.

AFM QNM has the additional capability that it receives information about parameters as topography, adhesion and Young's modulus in the same location. The results can then be presented individually or overlaid e.g. as topographic images with adhesion overlay or topographic images with Young's modulus overlay. Variations in adhesion and Young's modulus are observed at a nano to micrometer scale.

Figure 3 a shows a topographic image with an adhesion overlay and *Figure 3 b* shows a topographic image with a Young's modulus overlay for the bitumen sample "e" with wax content of 1.9 %, and refractive index of 1.579.

The adhesion forces measured in the region surrounding (peri phase) the 'bees' (catana phase) and the region in the 'bee' areas are lower than the adhesion force measured in the smooth matrix (para phase). Likewise it can be observed that Young's moduli in the region surrounding (peri phase) the 'bees' (catana phase) and in the 'bees' are higher than Young's modulus of the smooth matrix (para phase).

These Young's modulus results contradict the results presented by Dourado et al. (2011) who measured local stiffness variation via indentations on 50/70 bitumen binders and found that the bright areas of the bees presented a lower elastic modulus than the overall bee area, which in turn exhibited a lower elastic modulus than the matrix. The differences in the results may be explained by the fact that the 50/70 bitumen binder is a harder bitumen than the 70/100 bitumen binder. Another difference may be the temperature. If the bees contain wax, and the temperature of the binder is raised, Young's modulus of the bees may suddenly become lower than Young's modulus of the matrix.
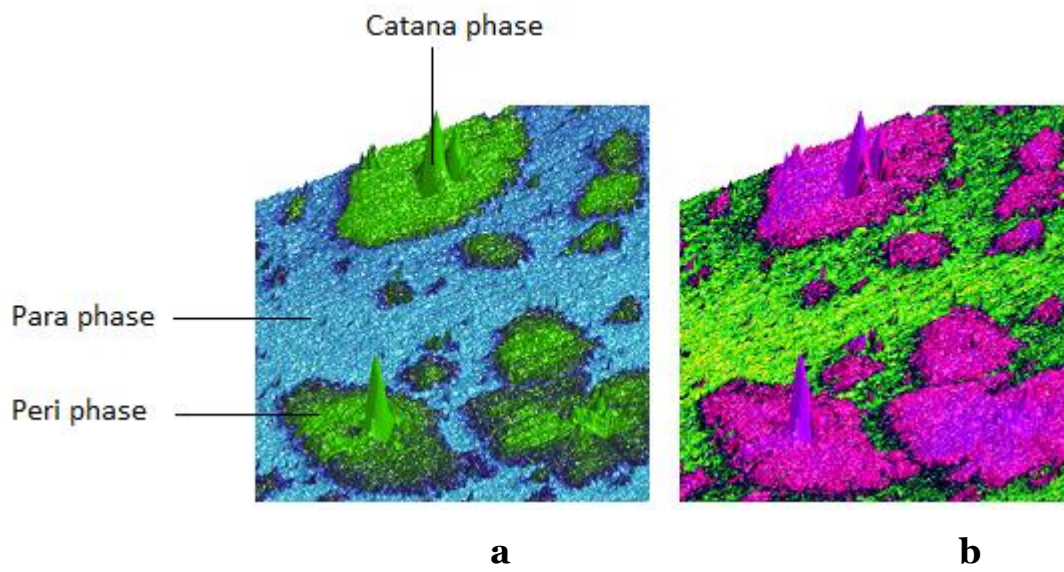
Figure 3 Sample "e" measured with AFM force mapping. (a): 3D Height zoom with adhesion overlay. (b): 3D Height zoom with Young's modulus overlay.

4.5   Surface Wrinkling: The Phenomenon Causing Bees in Bitumen

In this paper the mechanisms for bee formation are investigated. AFM QNM was used to investigate the microstructure on the surface of typical bitumen binders. Typical periodic topographic features resembling 'bee-like structures' or <u>catana phase</u> surrounded by a dispersed phase (<u>peri phase</u>) and the matrix can be observed in *Figures 4 a and b*. The higher and lower bands that constitute the bees continue from the bees out into the peri phase. This continuation of bands can also be seen in *Figure 4 b*. It is suggested here that the bee/catana phase and the peri phase are one single phase. Contrary to the classic understanding that there are two phases that make up the bees (catana) and its surrounding (peri), the authors suggest that the bees (catana) and the surrounding (peri) is a single phase. In this article, this combined phase (catana and peri) will be called the bee laminate phase.
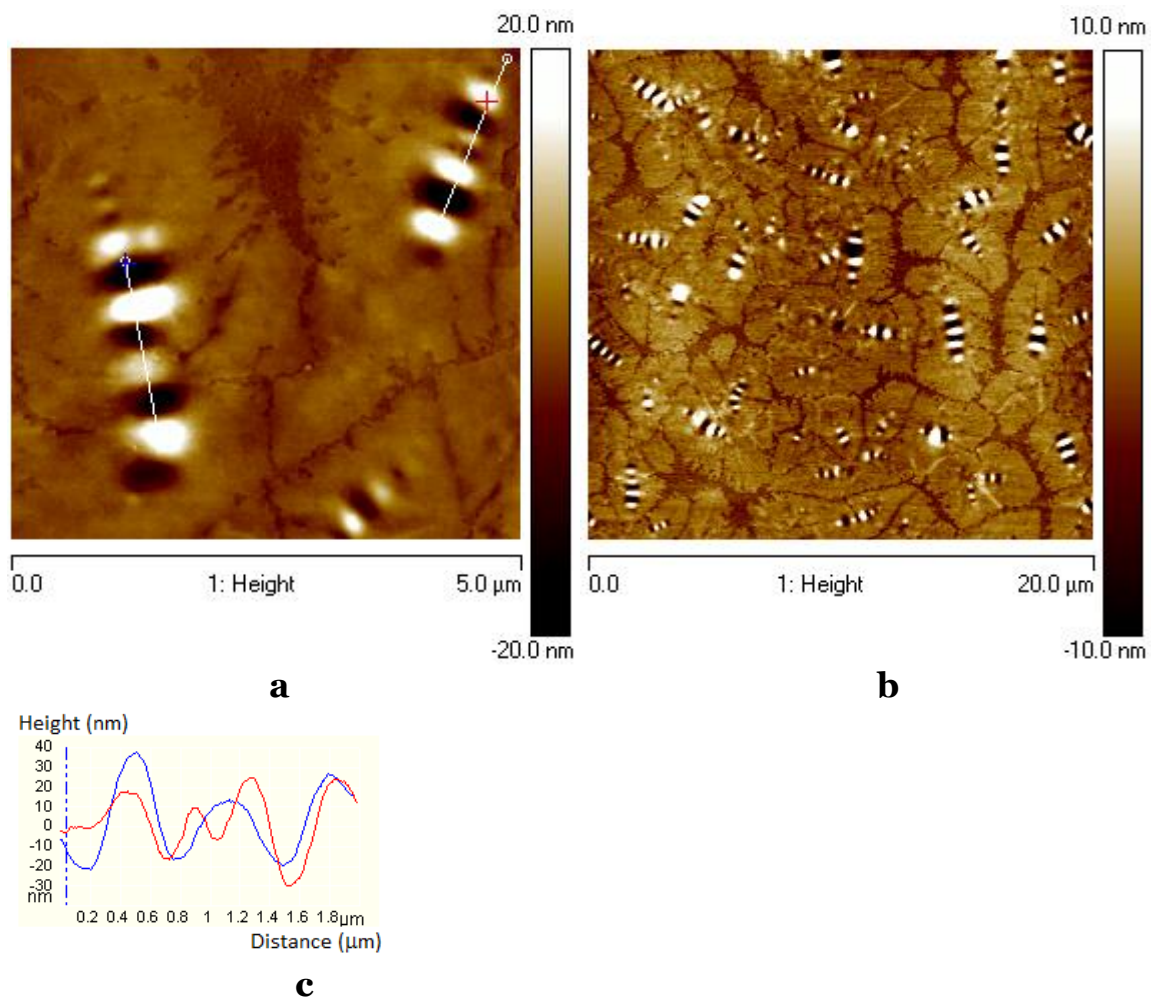

a   **b**

c

Figure 4   AFM QNM topography images of a penetration grade 70/100 bitumen binder.
a. x=5.0 μm   y=5.0 μm   z=0.04 μm
b. x=20.0 μm y=20.0 μm z=0.02 μm
c. Characteristic height lines (or profiles) of two bees.

AFM provides topographic information in the form of height lines (or profiles), i.e. the distance between the higher and lower parts of the bees (*Figure 4 c*). *Figure 4* shows two topographic images of the same bitumen binder with different resolutions. The x- and y- coordinates represent the dimensions in-the-plane and the z-coordinate represents the dimension out-of-the plane.

It is proposed here that the bee laminate phase is separated from the bulk and is transported to the surface of the bitumen just as chocolate sometimes 'blooms' due to the cocoa butter separating and migrating to the surface as a white haze (Longchamp and Hartel 2004).

What causes the bee laminate phase to look like bees?

A number of self-organized configurations can be found in nature from the organization of molecular structures to the organization of clusters in galaxies. Self-organization is normally initiated by internal variations.

One type of self-organization caused by internal variation is the spontaneous formation of highly ordered surface wrinkles (Chung, Nolte et al. 2011). These wrinkles are typically caused by thermal contraction, by moisture- or water leaving the material causing shrinkage, or by mechanical compression. Surface wrinkling is the result of the balance between the energy required to bend the stiffer bee laminate and the energy required to deform the softer matrix.

Consider the bee laminate consisting of a relatively thin material resting on a less stiff matrix (see *Figure 5*). Buckling-type instability of the thin surface material may then occur if this bee laminate is subjected to compressive loading, as during cooling of the bitumen from a melt. The thin bee laminate will start to wrinkle (due to buckling) with a defined wavelength and amplitude.
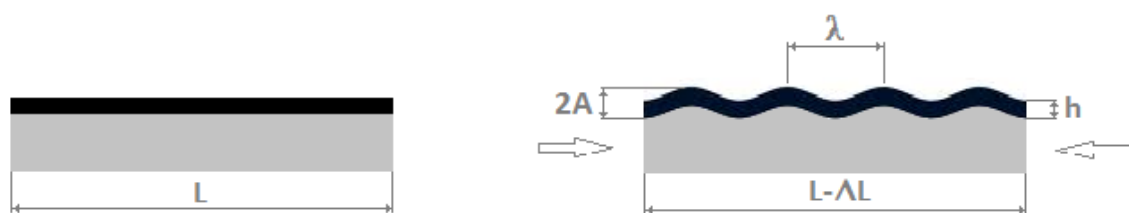

Figure 5   Schematic of surface wrinkling, adapted figure from Chung et al. (2011)**.**

The amplitude can be determined from the wavelength of the surface wrinkles and from material properties of the bee laminate phase and the matrix phase (Meredith, Karim et al. 2002). From observations of typical bees (such as in *Figure 4*) the

waveform of the buckled bee laminate is assumed to be sinusoidal, $(1 - v_m^2) \sim (1 - v_l^2)$, the critical wavelength can be determined by *Equation 17*:

$$\lambda = 2\pi h \left[\frac{(1-v_m^2)E_l}{3(1-v_l^2)E_m}\right]^{1/3} \sim 2\pi h \left[\frac{E_l}{3E_m}\right]^{1/3} \qquad (17)$$

where h is the thickness of the bee laminate, v is Poisson's ratio, E is Young's modulus, and subscripts *l* and *m* denote the bee laminate and the matrix phase.

The Young's moduli of the two phases are almost indistinguishable, though it would appear that the bee phase is systematically marginally higher than the matrix phase.

4.6   Obstacles to Measuring Bitumen Surface Energy as it Pertains to Adhesion in Asphalt

Penetration grade bitumen binders have been coated on glass slides and surface energy components have been determined from contact angle measurements using the sessile drop method (Bahramian 2012).

In this paper, surface energy components of these penetration grade bitumen binders were compared with surface energy components of probe liquids from the literature.

This comparison indicates that surface energy has actually been measured on the phase separated wax (or lower surface energy fraction) on the surface of the coated glass slide rather than the bulk phase. The sessile drop method is a technique to determine surface energies of solids and liquids. If bitumen phase separates, and the measurements are performed on the surface only, these measurements will not give representative values for the surface energy of the bulk of the bitumen material that adheres to minerals and aggregates.

The bitumen components that are expected to migrate to the air interface and to the surface of laboratory glass slides (or to the surface of aggregates) (see *Figure 6*) are identified based on the dielectric spectroscopic response of the material components, as reflected by their dielectric constants and refractive indices.
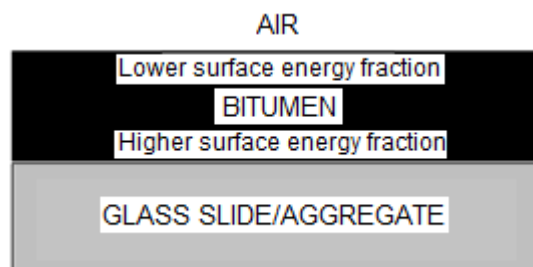

Figure 6   Surface energy fractions of bitumen in contact with air, and in contact with glass slide / aggregate.

Polarizability

The effective polarizability of an atom changes when it is surrounded by other atoms (Israelachvili 1991). The dielectric constant and the refractive index (as measures of two dominant types of polarizabilities) are discussed separately here due to the difficulty of enumerating the interaction energies for aggregates and large aromatic bitumen molecules.

Total polarizability

The total polarizability according to the Clausius-Mossotti equation (see *Equation 8*) can be determined from the dielectric constant of a material (Israelachvili 1991).

The total polarizability at zero-frequency only equals zero when the dielectric constant is 1. By definition, vacuum has a dielectric constant of 1. For such a material, only London dispersive polarizability is relevant. However with increasing dielectric constant, the degree of total polarizability will increase.

Solvents and polymeric materials with low and high molecular weights. The dielectric constant of low molecular weight solvents and high molecular weight polymeric materials are summarized in *Tables 5 and 6*. Note that the solvents and materials presented in *Tables 5 and 6* do not exist in bitumen. Non-polar functional groups in bitumen are associated with hydrocarbon groups that contain only carbon and hydrogen. It can be observed in *Tables 5 and 6* that the dielectric constant of materials and solvents with only non-polar functional groups is below approximately 3 indicating a low degree of total polarizability.

The dielectric constant of materials and solvents containing functional groups with oxygen and nitrogen is above approximately 3 indicating their higher degree of total polarizability.

As seen in *Tables 5 and 6*, the dielectric constant is a measure of degree of electronegativity, indicated by type of polar functional group. The solvents with the much smaller molecular weights in *Table 5* have dielectric constants in the same range as the materials in *Table 6* that have much larger molecular weights.

Solvents and polymeric materials containing molecules with a large degree of electronegativity difference also interact through hydrogen bonding and polar bonding. These solvents and materials have *in general* high dielectric constants and do not exist in non-aged bitumen. Alcohols, acids and water are examples of solvents with high dielectric constants.

Bitumen, asphaltenes, glass, and aggregates. The dielectric constant at 1000 Hz was determined for bitumen binders *A to G* and varied between 3.2 to 3.9 (Lyne et al. 2014b). The total polarizability is low for bitumen as a whole due to its low dielectric constant just slightly above 3. A dielectric constant of 3 indicates that bitumen consists mainly of molecules with non-polar functional groups.

In the literature, the dielectric constant of asphaltenes (or the n-heptane insoluble fraction) has been reported to be 5-7 (Oudin 1970; Maruska and Rao 1987). Dielectric constant values of asphaltenes are higher than those for bitumen as a whole.
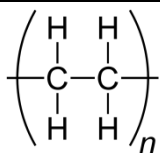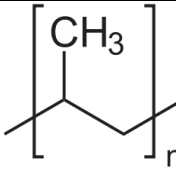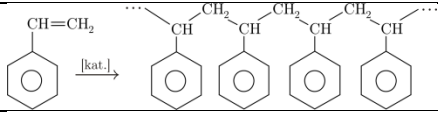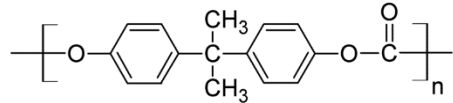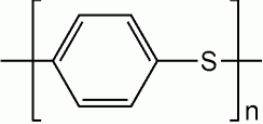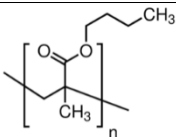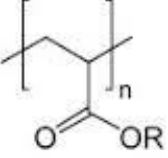
Typical aggregates in asphalt have dielectric constants in the range of 4 to 8. For example, the dielectric constant of a typical quartz is 4.2-5 (Telford et al. 1990), whereas calcite has a dielectric constant of approximately 8 (Rao and Rao 1968). The dielectric constant of glass is in the range of ε= 4-10, and the dielectric constant of vacuum is ε=1.

Table 5   Dielectric constant of (low molecular weight) solvents.

Solvent	Functional groups	ε	Ref.
n-heptane	Straight chain alkane	1.9	(Wikipedia 2014)
Ethyl benzene	Functionalized arene with ethyl group	2.3	(Microcat 2014)
0-Xylene	Functionalized arene with alkyl groups	2.3	(King 2013)
Toluene	Functionalized arene with alkyl group	2.4	(Wikipedia 2014)
Hexyl acetate	Functionalized ester with alkyl group	4.4	(Kokosa 2009)
Cyclohexyl-amine	Functionalized cyclohexane with aliphatic amine group	4.6	(Microcat 2014)
Methyl benzoate	Functionalized arene with ester group	6.6	(Rafoeg 2014)
Tetrahydro-furan	Functionalized cyclopentane with ether group	7.6	(Macro 2014)
Benzophenone	Functionalized arenes with a ketone in between	13	(Exvacuo 2014)
Cyclohexanone	Functionalized cyclohexane with ketone	18.3	(Microcat 2014)

The dielectric constant of asphaltenes (ε= 5-7), aggregates (ε= 4-8), and glass slides (ε= 4-10) are all higher than for materials with only non-polar functional groups (see *Tables 5 and 6*). This indicates higher degree of total polarizability for these materials compared to bitumen. None of these materials have a high dielectric constant as in being strongly polar. Thus, they are to different degrees Keesom and Debye polarizable.

Table 6   Dielectric constant of polymeric (high molecular weight) materials.

Material	Repeating unit	Molecular formula	ε	Ref.
Polyethylene		$(C_2H_4)_nH_2$.	2.3	(Lanza and Herrmann 1958)
Polypropylene		$(C_3H_6)n$	2.2	(Anderson and McCall 1958)
Polystyrene		$(C_8H_8)_n$	2.4-3.0	(Csgnework 2014)
Polycarbonate			2.8	(Rabuffi and Picci 2002)
Polyphenylenesulfide			3.0	(Rabuffi and Picci 2002)
Polyester			3.3	(Rabuffi and Picci 2002)
Poly (n-nutyl methacrylate)			4.28	(Havriliak and Negami 1967)
Polyacrylate		$(CH_2=CHCO_2R)$	6.5	(Havriliak and Negami 1967)

London dispersive (electronic) polarizability

The non-polar London dispersive (electronic) polarizability according to the Lorenz-Lorentz equation, i.e. the polarizability in the optical/UV spectrum, can be determined from the refractive index of a material (Israelachvili 1991)**,** see *Equation 7.*

Refractive index of bitumen binders **A** to **G** has been reported to 1.55 to 1.60 (Lyne et al. 2013b). These values can be compared to refractive indices of some common low and high molecular weight solvents and polymeric materials that are summarized in

Table 7. Note that the solvents and polymeric materials presented in *Table 7* are not found in bitumen.

The high refractive index of bitumen indicates its high London dispersive (electronic) polarizability which is a measure of the content of large aromatic molecules. The degree of the non-polar London dispersive polarizability increases with increasing molecular size and with increasing aromaticity, as seen in *Table 7.* Aromatic compounds are cyclic compounds in which all ring atoms contribute to a network of pi-pi interactions. The electron density of the network of the pi-pi interactions in aromatic compounds contributing to dispersive (electronic) polarizability is distributed above and below the rings. Aromatic molecules are able to interact with each other in so-called pi-pi-stacking. Aromatic molecules display enhanced chemical stability compared to non-aromatic molecules.
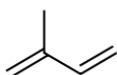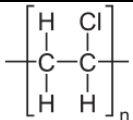
In the literature, the refractive index of asphaltenes (n-heptane insoluble fraction) has been reported to be 1.68 (Maruska and Rao 1987). This indicates that asphaltenes are highly London dispersive (electronic) polarizable. The higher London dispersive polarizability reflects primarily the higher degree of aromaticity (low weight-percent hydrogen) and the larger molecular weight of asphaltenes compared to the other fractions.

The refractive index increases with the size of the molecule, and hence the number of electrons. As shown by Hough and White (1980), values for the refractive index increase with increasing length of the alkane chain.

Phase separating wax molecules (or the lower surface energy phase) that may exist in bitumen have lower refractive indices than typical bitumen molecules and they normally belong to the lower range of molecular weights in bitumen.

The variation in refractive indices of typical aggregates used in asphalt pavements is quite significant. For example, refractive index of typical quartz is about 1.55, the refractive index of calcite is 1.68 and the refractive index of augite is 1.77 (WebMineral 2014). These numbers can be compared with the refractive index of bitumen as a whole having values in the range of 1.55-1.60. Asphaltenes are only a small fraction of bitumen but have a refractive index in the range of 1.68.

Table 7   Refractive index of solvents and materials.

Molecule	Functional groups	n	Ref.
Low molecular weight			
Methanol	CH_3OH	1.329	(Israelachwili 1991)
Ethanol	C_2H_5OH	1.361	(Israelachwili 1991)
n-heptane	$H_3C(CH_2)_5CH_3$ or C_7H_{16}	1.387	(Wikipedia 2014)
Hexanol	$n\text{-}C_6H_{13}OH$	1.418	(Israelachwili 1991)
Benzene	C_6H_6	1.501	(Israelachwili 1991)
Phenol	C_6H_5OH	1.551	(Israelachwili 1991)
High molecular weight			
Polyisoprene		1.502	(Hough and White 1980)
Polyvinylchloride		1.527	(Hough and White 1980)
Polystyrene	Se above	1.557	(Hough and White 1980)
Polystyrene	Se above	1.564	(Hough and White 1980)

4.7   Low Frequency Dielectric Spectroscopy of Bitumen Binders

The objective of this paper is to investigate the adhesion of un-aged penetration grade bitumen binders by means of permittivity analysis.

In the literature, the dielectric response of bitumen has been studied and documented by a number of authors:

The conductivity of fractions from the Athabasca bitumen show that heptane insoluble fraction (i.e. asphaltenes) has the highest conductivity of all the fractions (i.e. heptane insoluble fraction > resins, maltenes) (Penzes and Speight 1974).

The conductivity and dielectric response of several bitumens were studied as a function of their concentration in toluene at 1 kHz (Chow et al. 2004). The results illustrate that conductivity is dependent upon the n-heptane insoluble fraction of bitumen. The magnitude of the contribution to the overall dielectric constant was as follow: n-heptane insoluble fraction > resins > aromatics > saturates.

The dielectric response of four dissolved n-heptane insoluble fractions from four different crude oils and one resin have been analyzed in the frequency range of 0.01 to 1000 Hz (Vrålstad et al. 2009). The n-heptane insoluble fractions and resin were dissolved in toluene and the dielectric response of the solutions was measured at different concentrations. Vrålstad et al. (2009) observed low frequency dispersion (LFD) according to (Linhjell et al. 2009) in the real and imaginary parts of the complex relative permittivity at low frequencies. At the same concentration the n-heptane insoluble fractions showed a significantly higher LFD than the resin fraction. Vrålstad et al. (2009) attributed the LFD to the deposition of a capacitive layer of asphaltenes on the electrodes.

In this study, the measurements were performed on binders directly (not on binders in a specific solution). In the frequency range where LFD occurs, the molecules have 10 to 100 seconds to reorient and move before the current switches direction. In that time period, small to large molecules have had time to reach equilibrium before the field changes direction again contributing to the dielectric loss that is a dielectric material's inherent dissipation of electromagnetic energy into heat.

According to the literature, the n-heptane insoluble fraction has a larger tangent of the dielectric loss angle at low frequencies than other bitumen components. The refractive index of n-heptane insoluble fractions reported in the literature is higher than for bitumen as a whole. The dielectric constant is somewhat higher for the n-heptane insoluble fraction than for bitumen as a whole. The size of n-heptane insoluble fraction molecules renders them more highly London dispersive (electronic) polarizable. The total polarizability of the n-heptane insoluble fraction is somewhat

higher than that of the average of molecules in bitumen binders (i.e. bitumen as a whole). A high polarizability is a prerequisite for the bitumen binder to adhere well to stone aggregates.

Surface coverage by rolling bottle experiments

In a recent study, surface coverage (as a measure of adhesion) was investigated on the same bitumen binders by using the rolling bottle method where percentage bitumen adhering to quartzite aggregates was determined after 24 hours agitation in water (Olsson et al. 2010). Surface coverage was measured at two different laboratories, Lab A and Lab B.

Without any adhesion promoter added to the bitumen-aggregate mix, surface coverage was essentially non-existent (see *Table 8*). Portland cement was therefore added to the aggregate surface to improve the surface coverage (i.e. adhesion).

Table 8   Surface Coverage and Average tan δ (0.01 to 1 Hz).

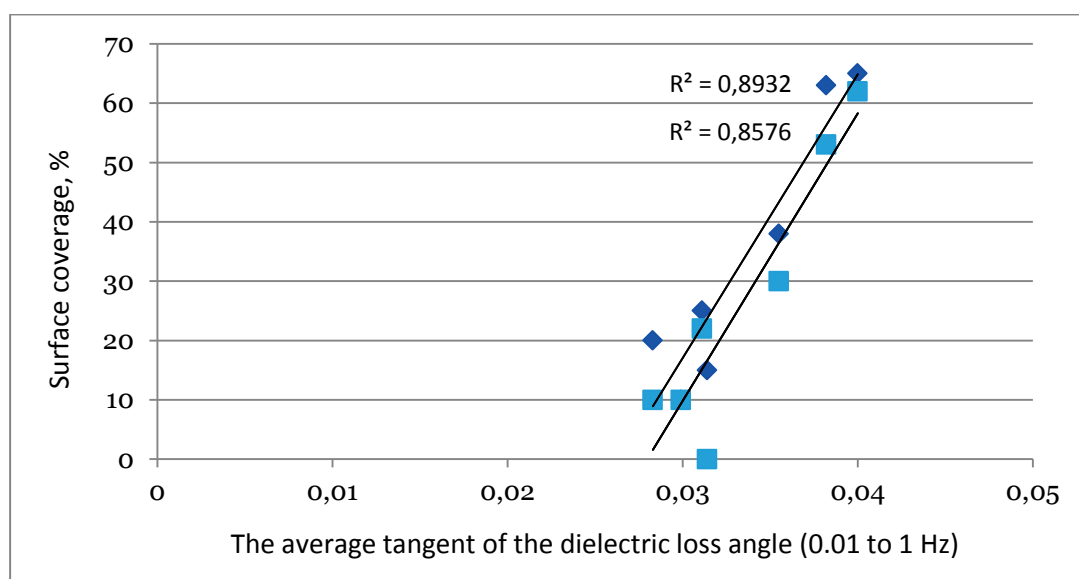| Laboratory A		Laboratory B		Average tan δ (0.01 to 1 Hz)
Reference	With cement	Reference	With cement	
0	10	0	10	0.0299
0	20	0	10	0.0283
0	63	0	53	0.0382
0	25	0	22	0.0311
0	38	0	30	0.0355
0	15	0	0	0.0314
5	65	0	62	0.0400

Figure 7   Surface coverage as a function of the average tangent of the dielectric loss angle.

With the addition of the Portland cement, surface coverage increased but to a different extent for each binder. It was possible to obtain a good linear fit between the average tangent of the dielectric loss angle, (in the frequency range of 0.01 to 1 Hz) and the surface coverage using the rolling bottle method (coefficient of determination 0.89 for Lab A and 0.86 for Lab B), see *Figure 7*. Average loss tangent in the frequency region of 0.01 to 1 Hz correlated well with the surface coverage data from the rolling bottle experiments. Bitumen binders having a higher average loss tangent in the frequency region of 0.01 to 1 Hz display higher surface coverage.

Without the addition of Portland cement to the surface of the quartz aggregate, bitumen is directly in contact with the quartz aggregate (see *Figure 8*). With the addition of Portland cement to the quartz aggregate, an intervening layer is placed between the bitumen binder and the quartz aggregate.
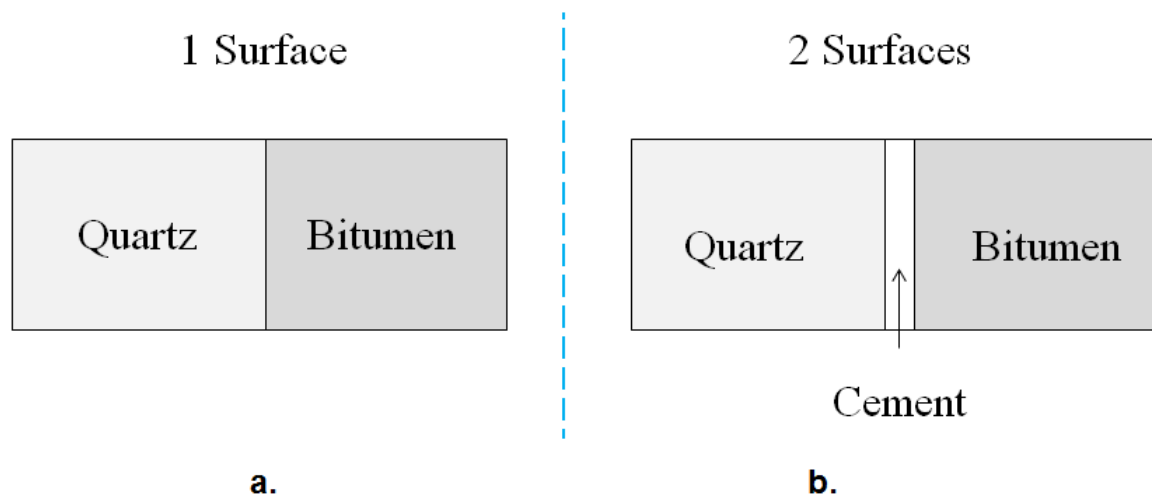

Figure 8   a. Quartz-Bitumen interaction, b. Quartz-Cement-Bitumen interaction.

As seen in *Table 9*, quartz (i.e. SiO_2) has a 'low' refractive index of 1.55 and a 'low' dielectric constant of 4.2. From these values it can be concluded that pure quartz has a lower London dispersive polarization (in comparison with other minerals) and a low total polarization. The interaction between quartz and bitumen can therefore be considered primarily London dispersive.

A typical Portland cement contains 63 percent calcium oxide, 1.5 percent magnesium oxide and 3 percent iron oxide (Neville and Brooks 1987). MgO has a high refractive index of 1.74 and a high dielectric constant of 9.90, CaO has a high refractive index of 1.84 and a high dielectric constant of 11.95, and iron oxides have even higher refractive index of w=2.11-2.73 (depending on iron oxide type) and an even higher dielectric constants of 20.6 and 31.4 (also depending on iron oxide type) (WebMineral 2014).

MgO, CaO and iron oxides all have high refractive indices indicating their high degree of London dispersive polarizability. All oxides have also high dielectric constants, especially iron oxides, indicating their high degree of total polarizability. Portland cement is a material strongly contributing to Debye and Keesom interactions. The higher surface coverage with the addition of the Portland cement on the surface of the aggregates can be explained by the higher London dispersive polarizability of Portland cement and the higher total polarizability of the MgO, CaO and iron oxides. When Portland cement is added to asphalt (to the surface of the aggregates) it is known to improve adhesion between bitumen and several types of aggregates, as reflected here by improved total and dispersive polarizabilities.

The dielectric constant of iron oxides is as high as some polar compounds and solvents such as acetone (20.7) and ethanol (24.3). The reactivity of iron oxides may also add to bonding to aggregates and to bitumen.

Table 9   Refractive indices and dielectric constants of oxides.

Oxides	Refractive Index (1)	Dielectric Constant
SiO_2 (Quartz)	w=1.543-1.545 e=1.552-1.554	4.2 (2)
MgO	1.74	9.90 (3)
CaO	1.84	11.95 (3)
-Iron(II) oxide (FeO) -Iron(III) oxide (Fe_2O_3) also known as hematite, occurs in the mineral magnetite.	2.11, 2.13 (FeO) 2.54, 2.73 (Fe_2O_3)	w=24, e=31.4 (FeO) (4) w=20.6, e=24.1 (Fe_2O_3) (4)

(1) (WebMineral 2014)
(2) (Kim et al. 2001)
(3) (Subramanian et al. 1989)
(4) (Kück et al. 2000)

5 Conclusions

This thesis deals with the interactions of bitumen binders and aggregates / minerals in asphalt pavements.

Hamaker's constant (Paper I-III)

Paper I: The stripping performance of aggregates and minerals correlates well to Hamaker's constant.

Paper II: Refractive index can be used to estimate the dispersive component of adhesion of minerals to bitumen. It is clear from this study that the elemental composition of a mineral will affect its refractive index and hence its dispersive adhesion to bitumen. Higher dispersive interactivity of minerals can be derived from the presence of specific elements in the mineral. Comparison with known mineral and aggregates stripping sensitivity has given an empirical cut off level at a refractive index of 1.6. Minerals containing alkali metals tend to have a low dispersive interaction with bitumen indicated by a refractive index below 1.6. Minerals that include transition metals tend to have high refractive index and higher dispersive interaction. A higher percentage of magnesium, calcium and aluminum promotes higher refractive indices and higher dispersive interactions. Minerals can have a higher refractive index due to the occurrence of specific elements in the mineral, but still have poor adhesion due to the presence of alkali metals.

Paper III: Refractive indices of aggregates are the average of the composite minerals which in turn depend on the specific elements in the minerals. Refractive indices of bitumen binders are the average of constituent components and it will depend on the specific elements in the binder. Comparison with known mineral stripping sensitivity has given an empirical cut off level for refractive index of 1.6. This can now be explained by the following: if the aggregate has a higher refractive index than 1.6, cohesive failure is likely to occur, i.e. adhesion failure is not likely to occur. If the aggregate has a refractive index of the same magnitude as the bitumen binder, then failure due to lack of strength of adhesion will be as likely as cohesive failure within the bitumen binder.

Topographic Morphologies of Bitumen Binders (Paper IV-V)

Paper IV: The surface force mapping technique, AFM QNM, was used to measure topography, adhesion and elastic modulus simultaneously on un-aged 70/100 penetration grade bitumen binders. The adhesion forces measured in the region surrounding the periodic topographic features resembling 'bees' and the region in

the 'bee' areas are lower than the adhesion force measured in the smooth matrix. Likewise it can be observed that Young's moduli in the region surrounding the 'bees' and in the 'bees' are higher than the Young's modulus of the smooth matrix. The bee phase is believed to consist of wax since wax is stiffer than bitumen at room temperature.

Paper V: The mechanism for bee formation was also investigated via AFM. Bees are a phenomenon caused by phase separation, where the phases have different rigidities and different thermal expansion coefficients resulting in differential shrinkage during cooling and ridging (interchanging higher and lower bands in the topographic surface).

Bitumen-Aggregate Adhesion (Papers VI and VII)

Paper VI: Penetration grade bitumen binders were coated on glass slides and surface energy components were determined from contact angle measurements using the sessile drop method. Surface energy components obtained were compared with surface energy components of probe liquids from the literature. This comparison indicates that surface energy has actually been measured on the phase separated wax on the surface of the coated glass slide rather than the bulk phase. The sessile drop method is a technique to determine surface energies of solids and liquids. If bitumen phase separates, and the measurements are performed on the surface only, these measurements will not give representative values for the surface energy of the bulk of the bitumen material that adheres to minerals and aggregates.

This study is limited to two dominant adsorption frequencies/frequency regions. The total polarizability at zero-frequency, can be determined from the dielectric constant. The non-polar London dispersive (electronic) polarizability in the optical/UV spectrum, can be determined from refractive index measurements. In materials with higher permittivity at zero frequency the Keesom and Debye attraction energies will be responsible for a significant part of the polarization.

Bitumen as a whole has a low degree of total polarizability. Bitumen contains a small fraction of n-heptane insoluble molecules that have a somewhat higher total polarizability.

Bitumen as a whole is highly London dispersive (electronic) polarizable and the asphaltene (or n-heptane insoluble) fraction is even higher London dispersive (electronic) polarizable. The degree of non-polar London dispersion polarizability increases with increasing molecular size and with increasing aromaticity.

Neither un-aged bitumen, asphaltenes, glass nor typical aggregates used in asphalt pavements have high dielectric constants. Thus, they are to different degrees Keesom and Debye polarizable.

Paper VII: The initial adhesion of non-aged bitumen binders to pure quartz aggregates is primarily London dispersive (electronic) polarizable due to low total polarizability of the components. Bitumen contains a small fraction of n-heptane insoluble molecules that have a somewhat higher total polarizability and therefore may contribute to Debye and Keesom interactions.

The higher surface coverage with the addition of the Portland cement on the surface of the aggregates can be explained by higher London dispersive polarizability and higher total polarizability of CaO, MgO and iron oxides. Portland cement is a material contributing to Debye and Keesom interactions. Portland cement could also have chemical influence on its bonding to aggregates.

A strong correlation was identified between the average tangent of the dielectric loss angle in the frequency region of 0.01 to 1 Hz and surface coverage (a common method to indicate suitability of bitumen for use in roads). Surface coverage is higher for bitumen binders having a larger average loss tangent.

It is suggested that the average tangent of the dielectric loss angle in the frequency range of 0.01 to 1 Hz, could be used as an indicator for predicting polarizability and thereby, adhesion potential of bitumen binders.

6   Recommendations

The main aim of this doctoral thesis was to propose a hypothesis for what makes bitumen binders stay adhered to aggregates (or filler particles such as Portland cement) and to provide a fundamental understanding for the development of a new test method for bitumen-aggregate adhesion.

The proposed hypothesis is based on neither bitumen nor aggregates being homogenous materials. The bitumen to aggregate adhesion therefore depends on constituent minerals in the aggregate and constituent fractions in the bitumen binder. It is recommended that the proposed mechanism should be further validated by additional physical and chemical testing. Secondly, the consequences of aging and how it affects the material properties of the bitumen binder and the aggregate should be taken into consideration.

Thirdly, realizing that the asphaltene fraction (n-heptane insoluble fraction) is disproportionally important for polarizability it would have been good to measure the dielectric properties (dielectric constant and refractive index) of the asphaltene

fractions from the actual bitumen samples used in this study, rather than taking literature values.

Lastly, the average tangent of the dielectric loss angle in the frequency region of 0.01 to 1 Hz was found to relate well to surface coverage (a common method to indicate suitability of bitumen for use in roads). Surface coverage is higher for bitumen binders having a larger average loss tangent. A greater proportion of large molecules renders compounds highly polarizable primarily due to the London dispersive (electronic) polarizability but also to somewhat higher total polarizability. It is recommended that this mechanism be studied further with a view to optimizing bitumen composition for promoting roads that are more durable.

7   Bibliography

Anderson, E. W. a. M., D.W. (1958). "The dielectric constant and loss of polypropylene." Journal of Polymer Science 31(122): 241-242.

Applequist, J. (1993). 'Atom charge transfer in molecular polarizabilities: application of the Olson-Sundberg model to aliphatic and aromatic hydrocarbons.' Journal of Physical Chemistry 97(22): 6016-6023.

Arvidsson,H. and Loorents, K.-J. (2008). 'Inverkan av köld och vatten på glimmerhaltiga bärlag.' VTI notat 2-2008. www.vti.se/publikationer.

Bagampadde, U., Isacsson, U. and Kiggundu, B.M. (2004). 'Classical and Contemporary Aspects of Stripping in Bituminous Mixes – State of the Art.' Road Materials and Pavement Design, 5(1)7-43.

Bagampadde, U. (2005). "Investigations on moisture damage-related behaviour of bituminous materials." Doctoral Thesis in Highway Engineering, KTH Royal Institute of Technology, Stockholm, Sweden.

Bagampadde, U., Isacsson, U. and Kiggundu, B.M. (2006). 'Influence of aggregate chemical and mineralogical composition on stripping in bituminous mixtures.' The International Journal of Pavement Engineering 6, 4, 229-239.

Bahramian, A. (2012). 'Evaluating surface energy components of asphalt binders using Wilhelmy plate and sessile drop techniques.' Master's thesis. Royal Institute of Technology. Stockholm, Sweden.

Binning, G., Quate, C. F. and Gerber, C. (1986). 'Atomic Force Microscopy.' Physical Review Letters 56(9): 930-933.

Britannica (2014). 'Dielectrics'. Retrieved 2014-01-09.

Buckley, J. S. (1996). 'Microscopic Investigation of the Onset of Asphaltene Precipitation.' Fuel Science and Technology International 14: 55-74.

Buckley, J. S., Hirasaki, G.J., Liu, Y., Von Drasek, S., Wang, J-X., and Gill, B.S (1998). 'Asphaltente precipitation and solvent properties of crude oils. 'Petroleum Science and Technology.' 16 3-4: 251-285.

Carambassis, A., Jonker, L. C., Attard, P. and Rutland, M.W. (1998). 'Forces measured between hydrophobic surfaces due to a submicrocopic bridging bubble.' Physical Review Letters 80(24): 5357-5360.

Chen, L.F., Ong, C.K., Neo, C.P., Varadan, V.V., and Varadan, V.K. (2004). 'Microwave electronics: measurement and materials characterization.' John Wiley and Sons.

Chisholm, Hugh, Ed (1911). 'Petrology.' Encyclopedia Britannica. Eleventh edition. Cambridge University Press.

Chow, R. S., Tse, D.L., Takamura, K. (2004). 'The conductivity and dielectric behaviour of solutions of bitumen in toluene.' Canadian Journal of Chemical Engineering 82: 840-845.

Chung, J. Y., Nolte, A.J., and Stafford, C.M. (2011). 'Surface wrinkling: A Versatile Platform for Measuring Thin-Film Properties.' Advanced Materials 23: 349-368.

Cordon, W.A. (1979). 'Properties, Evaluation, and Control of Engineering Materials.' McGraw-Hill, N.Y.

Csgnetwork (2014). http://www.csgnetwork.com/dieconstantstable.html 2014-05-14.

Dahlenborg, H., MiA., Bergenståhl, B. and Kalnin, D.J.E. (2011). 'Investigation of chocolate surfaces using profilometry and low vacuum scanning electron microscopy.' Journal of the American Oil Chemists Society 88: 773-783.

de Moraes, M. B., Pereira, R.B., Simao, R.A., and Leite, L.F.M. (2010). 'High temperature AFM study of CAP 30/45 pen grade bitumen.' Journal of Microscopy. 239(1): 46-53.

Derjaguin, B. V., Muller, V.M., and Toporov, Yu.P. (1975). 'Effect of contact deformations on the adhesion of particles.' Journal of Colloid and Interface Science 53(2): 314-326.

Dourado, E. R., Simao, R.A., and Leite, L.F.M (2011). 'Mechanical properties of asphalt binders evaluated by atomic force microscopy.' Journal of Microscopy 245: 118-119.

Ensley, E.K. (1975). 'Multilayer Adsorption with Molecular Orientation of Asphalt on Mineral Aggregate and Other Substrates.' Journal of Applied Chemistry and Biotechnology, 25, 671-682.

Ensley, E.K., Petersen, J.C. and Robertson, R.E. (1984). 'Asphalt-Aggregate Bonding Energy Measurements by Microcalorimetric Methods.' Thermochimica Acta, 77, 95-107.

Fantner, G. E., Oroudjev, E., Schitter, G., Golde, L.S., Turner, P., Finch, M.M., Turner, P., Gutsmann; T., Morse, D.e., Hansma, H., and Hansma, P.K. (2006). 'Sacrificial bonds and hidden length: unraveling molecular mesostructures in tough materials.' Biophysical Journal 15: 1411-1418.

Fowkes, F.M., (1962). 'Determination of Interfacial Tensions, Contact Angles and Dispersion Forces in Surfaces by Assuming Additivity of Intermolecular Interactions in Surfaces.' Journal of Physical Chemistry, 66(2)382.

Fromm, H.J. (1974). 'The mechanics of asphalt stripping from aggregate surfaces.' Ontario Ministry of Transportation and Communication.' Research Rapport 190.

Ghosh, V., Ziegler, G.R., and Anantheswaran, R.C. (2002). 'Fat, moisture, and ethanol migration through chocolates and confectionary coating.' Critical Reviews in Food Science and Nutrition 42: 583-626.

Goual, L., and Firoozabadi, A. (2002). "Measuring asphaltenes and resins, and dipole moment in petroleum fluids." AlChE Journal 48(11): 2646-2663.

Hamaker, H. C. (1937). 'The London-van der Waals Attraction Between Spherical Particles.' Physica 4(10): 1058-1072.

Handbook of Mineralogy (2011). [Electronic]. Available: http://www.handbookofmineralogy.org/search.html?p=alpha [2011-03-08].

Havriliak, S. a. N., S. (1967). "A complex plane representation of dielectric and mechanical relaxation processes in some polymers. ." In Polymers. Elsevier 8: 161-210.

Hefer, A., and Little, D.N (2005). 'Adhesion in Bitumen-Aggregate Systems and Quantification of the Effects of Water on the Adhesive Bond. International Center for Aggregates Research.' Research Report ICAR-505-1.

Hough, D. B., and White, L. R (1980). 'The calculation of Hamaker constants from Lifshitz theory with applications to wetting phenomena.' <u>Advances in Colloid and Interface Science</u> 14: 3-41.

Höbeda, P. (1998). 'Vattenkänslighet hos asfaltbeläggning. En litteraturutredning.' (In Swedish). National Road and Traffic Research Institute, Linköping, Sweden. <u>VTI</u> <u>Internal</u> <u>Rapport</u> No. 35.

Höbeda, P. and Thorèn, H. (1975). 'Berggrundens vägbyggnadstekniska egenskaper.' (In Swedish). National Road and Traffic Research Institute, Linköping, Sweden. <u>VTI</u> <u>Internal</u> <u>Rapport</u> No. 221.

Iler R.K., (1979). The chemistry of silica. Wiley, New York. P. 623-729.

Isacsson, U. (1976). 'Vidhäftning i bituminösa beläggningar. En litteraturutredning.' (In Swedish). National Road and Traffic Research Institute, Linköping, Sweden. <u>VTI</u> <u>Internal</u> <u>Rapport</u> No. 6.

Israelachvili, J. (1991). 'Intermolecular and Surface Forces.' <u>Academic Press</u>. Second Edition.

Jamieson, I.L., Moulthrop, J.S. and Jones, D.R. (1995). 'SHRP Results on Binder-Aggregate Adhesion and Resistance to Stripping.' Asphalt Yearbook 1995, 17-21. 26 <u>Road Materials and Pavement Design</u>. Volume 11 Special Issue. P. 305-323.

Jasperson, S. N., and Schnatterly, S. E (1969). 'An Improved Method for High Reflectivity Ellipsometry Based on a New Polarization Modulation Technique.' <u>The Review of Scientific Instruments</u> 40(6): 761-767.

Jones, D.R. (1992). 'Understanding How the Origin and Composition of Paving-Grade Asphalt Cements Affect their Performance.' SHRP, Asphalt Research Tech. Univ. of Texas at Austin, Texas. Memo. No. 4.

Jones, D.R. IV. (1993). 'SHRP Material Reference Library: Asphalt Cements: A concise Data Compilation.' SHRP-A-645, National Research Council, Washington DC.

Hansson, P. M., Swerin, A.,Schoelkopf, J., Gane, P.A.C., and Thormann, E. (2012). 'Influence of Surface Topography on the Interactions between Nanostructured Hydrophobic Surfaces.' <u>Langmuir</u> 28: 8026-8034.

Hough, D. B., and White, L. R (1980). 'The calculation of Hamaker constants from Lifshitz theory with applications to wetting phenomena.' <u>Advances in Colloid and Interface Science</u> 14: 3-41.

Huang, Y. H., Ed. (2004). 'Pavement Analysis and Design.' Upper Saddle River, NJ, USA, <u>Pearson Prentice Hall</u>.

Hutter, L. J., and Bechhoefer, J. (1993). 'Calibration of atomic force microscope tips.' <u>Review of scientific instruments</u> 64(7): 1868-1873.

Kané, M., Djabourov, M., Volle, J.-L., Lechaire, J.-P., and Frebourg, G. (2003). 'Morphology of paraffincrystals in waxycrudeoils cooled in quiescent conditions and under flow.' <u>Fuel</u> 82.(2.): 127-135.

King, C. J. (2013). <u>Separation processes</u>.

Kim, Y.-H., Hwang, M.S., and Kim, H.J. (2001). 'Infrared spectroscopy study of low-dielectric-constant fluorine-incorporated and carbon-incorporated silicon oxide films.' Journal of Applied Physics 90(7): 3367-3370. .

Kück, S., Werheit, H. Madelung, O. (Ed.) (2000). 'Non-Tetrahedrally Bonded Binary Compounds II, Landolt-Börnstein - Group III Condensed Matter.' Volume 41D.

Kokosa, J. M., Przyjazny, A., Jeannot, M.A. (2009). "Solvent Microextraction Theory and Practice ".

Lanza, V. L. a. H., D.B. (1958). "The density of the dielectric constant of polyethylene." Journal of Polymer Science 28(118): 622-625

Lifshitz, E. M. (1956). 'The Theory of Molecular Attractive Forces between Solids.' Soviet Physics JTP 2: 73-83.

Linhjell, D., Lundgaard, L. and Gäfvert, U. (2007). 'Dielectric Responce of Mineral Oil Impregnated Cellulose and the Impact of Aging.' IEEE Transactions on Dielectrics and Electrical Insulation 14(1): 156-169.

Little, D. N., and Bhasin, A (2006). 'Using Surface Energy Measurements to Select Materials for Asphalt Pavement.' Contractor's Final Report for NCHRP Project 9-37.

Loeber, L., Sutton, O., Morel, J., Valleton, J.-M., Muller, G (1996). 'New direct observations of asphalts and asphalt binders by scanning electron microscopy and atomic force microscopy.' Journal of Microscopy 182(1): 32-39.

Longchamp, P. and R. W. Hartel (2004). 'Fat bloom in chocolate and compound coatings.' European Journal of Lipid Science and Technology 106: 241-274.

Lu, X., and Redelius, P. (2006). 'Compositional and Structural Characterization of Waxes Isolated from Bitumens.' Energy and Fuels. 20: 653-660.

Lu, X., and Redelius, P. (2007). 'Effect of bitumen wax on asphalt mixture performance.' Construction and Building Materials. 21(11): 1961-1970.

Lu, X., Kalman, B., and Redelius, P (2008). 'A new test method for determination of wax content in crude oils, residues and bitumens.' Fuel 87: 1543-1551.

Lu, X., Langton, M., Olofsson, P., and Redelius, P. (2005). 'Wax morphology in bitumen.' Journal of Materials Science 40: 1893-1900.

Lyne, Å. L., Birgisson, B., and Redelius, R. Volume Special Issue (2010). "Interaction forces between mineral aggregates and bitumen calculated using the Hamaker constant." Road Materials and Pavement Design 11 (Special Issue): 305-323.

Lyne, Å. L., Collin, M., and Birgisson, B (2014a). "Obstacles to measuring bitumen surface chemistry as it pertains to adhesion in asphalt." Submitted to Journal of Materials Science.

Lyne, Å. L., Krivosheeva, O., and Birgisson, B. (2013b). "Adhesion between bitumen and aggregate - Implementation of spectroscopic ellipsometry characterisation and estimation of Hamaker's constant." Materials and Structures 46: 1737-1745.

Lyne, Å. L., Redelius, P., Collin, P. and Birgisson, B. (2013a). "Characterization of stripping properties of stone material in asphalt." Materials and Structures 46: 47-61.

Lyne, Å. L., Taylor, N., Jaeverberg, N., Edin, H. and Birgisson, B. (2014b). "Low frequency dielectric spectroscopy of bitumen binders." Submitted to Fuel.

Lyne, Å. L., Wallqvist, V., and Birgisson, B (2013c). "Adhesive surface characteristics of bitumen binders investigated by Atomic Force Microscopy." Fuel 113: 248-256.

Lyne, Å. L., Wallqvist, V., Rutland, M.W., Claesson, P., and Birgisson, B. (2013d). "Surface wrinkling: the phenomenon causing bees in bitumen." Journal of Materials Science 48(20): 6970-6976.

Mack, C. (1941). 'Study of bituminous mixtures on road-testing machines.' Journal of the Society of Chemical Industry Vol. 60, Issue 5, May.

Macro (2014). http://macro.Isu.edu/howto/solvents/THF.htm Retrieved 2014-01-27.

Majidzadeh, K. and Brovold, F.N. (1968). 'Effect of Water on Bitumen-Aggregate Mixtures.' Highway Research Board, Special Report 98.

Maruska, H. P., and Rao, B.M.L. (1987). 'The role of polar species in aggregation of asphaltenes.' Fuel Science and Technology International 5(2): 119.

Masson, J.-F., Leblond, V. and Margeson, J. (2006). 'Bitumen morphologies by phase-detection atomic force microscopy.' Journal of Microscopy 221: 17-29.

Masson, J. F., Leblond, V., Margeson, J., and Bundalo-Perc, S. (2007). 'Low temperature bitumen stiffness and viscous paraffinic nano and micro size domains by cryogenic AFM and PDM.' Journal of Microscopy. 227(3): 191-202.

Meredith, J. C., Karim, A., and Amis, E.J. (2002). 'Combinatorial methods for investigations in polymer materials science.' Material Research Society Bulletin 27: 330-335.

Microcat, C. (2014). http://www.microkat.gr/msdspd90-99/Cyclohexylamine.htm Retrieved 2014-01-27.

Microcat, C. (2014). http://www.microkat.gr/msdspd90-99/Cyclohexanone.htm 2014-01-27.

Microcat, E. (2014). http://www.microcat.gr/msdspd90-99/Ethylbenzene.htm. Retrieved 2014-01-27.

Miquel, M. E., Carli, S., Couzens, P.J., Wille, H.J., and Hall, L.D. (2001). 'Kinetics of the migration of lipids in composite chocolate measured by magnetic resonance imaging.' Food Research International 34: 773-781.

Mitchell, D. L., Speight, G (1973). 'The solubility of asphaltenes in hydrocarbon solvents.' Fuel 52(4): 149-152.

Muller, V. M., Derjaguin, B.V., and Toporov, Yu.P. (1983). 'On two methods of calculation of the force of sticking of an elastic sphere to a rigid plane.' Colloids and Surfaces 7(3): 251-259.

Musser, B. J., and Kilpatrik, P. K. (1998). 'Molecular characterization of wax isolated from a variety of crude oils.' Energy and Fuels 12: 715-725.

Naderi, A., Iruthayaraj, J., Vareikis, A., Makuska, R., Claesson, PM (2007). 'Surface properties of bottle-brush polyelectrolytes on mica: effects of side chain and charge densities.' Langmuir 23(24): 12222-12232.

Narayanamurti, V., Störmer, H.L., Chin, M.A., Gossard, A.C., Wiegmann, W (1976). 'Selective Transmission of High-Frequency Phonons by a Superlattice: The "Dielectric" Phonon Filter' Physical Review Letters 43(27): 2012-2016.

Neville, A. M., and Brooks, J.J. (1987). 'Concrete Technology.' Second Edition.

Nickel, E.H. (1995). 'The definition of a mineral.' The Canadian Mineralogist 33 (3): 689–690.

Olsson, K., Krona, N., and Nordgren, T (2010). 'Asphalt concrete test sections containing bitumen of different origins.' SBUF report 12091.

Oudin, J. L. (1970). 'Analyse Géochimique de la Matière Organique Extraite des Roches Sédimentaires I. Composés Extractibles au Chloroforme.' Rev. Ins. Fr. Pét. 25 (1): 4.

Owens, D. K., and Wendt, R.C. (1969). 'Estimation of the surface free energy of polymers.' Journal of Applied Polymer Science(13): 1741-1747.

Parsegian, V.A. (2006). 'van der Waals forces. A handbook for Biologists, Chemists, Engineers.' and Physicists, Cambridge University Press, First edition, 2006.

Pauli, A. T., Grimes, R.W. Beemer, A.G., Turner, T.F. and Brandhaver, J.F (2011). 'Morphology of asphalts, asphalt fractions and model wax-doped asphalts studied by atomic force microscopy.' International Journal of Pavement Engineering 12: 291-309.

Peltonen, P. (1992). 'Road aggregate choice based on silicate quality and bitumen adhesion.' Journal of Transportation Engineering, Vol. 118, No. 1.

Penzes, S., and Speight, J.G. (1974). 'Electrical conductivities of bitumen fractions in non-aqueous solvents.' Fuel 53: 192-197.

Pittenger, B., Erina, N., and Su, C. (2010) 'Quantitative Meachanical Property Mapping at the Nanoscale with PeakForce QNM'. Veeco Instruments Inc.

Plancher, H., Dorrence, S.M., and Petersen, J.C (1977). "Identification of chemical types in asphalts strongly adsorbed at the asphalt-aggregate interface and their relative displacement by water." Proc. Association of Asphalt Paving Technologists 46: 151-175.

Pople, S. and Williams, M. (2002). 'Science to GCSE.' Oxford University Press. Second edition.

Rabuffi, M. a. P., G. (2002). "Status quo and future prospects for metallized polypropylene energy storage capacitors " IEEE Transactions on plasma science 30(5): 1939-1942.

Rafoeg (2014). http://www.rafoeg.de/20.../20, Daten/dielectric_chart.pdf Retrieved 2014-01-27.

Rao, K. S., and Rao, K.V. (1968). 'Dielectric Dispersion and its Temperature Variation in Calcite Single Crystals.' Zeitschrift fir Physik 216: 300--306.

Read, J., and Whiteoak, D. (2003). Fifth edition. The Shell Bitumen Handbook.

Redelius, P.G. (2000). 'Solubility Parameters and Bitumen.' Fuel 79, 27-35.

Redelius, P., Lu, X., and Isacsson, U. (2002). 'Non-Classical Wax in Bitumen.' Road Materials and Pavement Design. 3(1): 7-21.

Redelius, P. G. (2006). 'The structure of asphaltenes in bitumen.' Road Material and Pavement Design (Special Issue): 143 - 162.

Saether, E. (1948). 'Om vedheftning mellom bituminöse bindemidler og steinmaterialer.' Meddelelser fra Vegdirektören, Nr. 1.

Schmets, A., Kringos, N., Pauli, T., Redelius, P. and Scarpas, T. (2010). 'On the existence of wax-induced phase separation in bitumen.' International Journal of Pavement Engineering 11(6): 555-563.

Smith, B. L., Schaffer, T.E., Viani, M., Thompson, J.B., Frederick, N.A., Kindt, J., Belcher, A., Stucky, G.D., Morse, D.E., and Hansma, P.K. (1999). 'Molecular mechanistic origin of the toughness of natural adhesives, fibres and composites' Nature 399(761-763).

Stafford, C. M., Harrison, C., Beers, K.L., Karim, A., Amis, E.J., VanLandingham, M.R., Kim, H.C., Volksen, W., Miller, R.D., and Simonyi, E.E. (2004). 'A buckling-based metrology for measuring the elastic moduli of polymeric thin films.' Nature Materials: 545-550.

Stuart, K.D. (1990). 'Moisture damage in asphalt mixtures – A state-of-the-art report.' Report No. FHWA-RD-90-019., Federal Highway Administration, Washington, D.C. (March 1990).

Subramanian, M. A., Shannon, R.D., Chai, B.H.T., Abraham, M.M., and M.C. Wintergill, M.C. (1989). 'Dielectric constants of BeO, MgO, and CaO using the two-terminal method.' Phys Chem Minerals 16: 741-746.

Taylor, S. D., Czarnecki, J., and Masliyah, J (2001). 'Refractive index measurements of diluted bitumen solutions.' Fuel 80(14): 2013-2018.

Telford, W. M., Geldart, L.P., and Sheriff, R.E. (1990). 'Applied Geophysics'. Cambridge University Press. Second Edition. P. 291.

Thompson, J. B., Kindt, J. H., Drake, B., Hansma, H.G., Morse, D.E., and Hansma, P.K. (2001). 'Bone indentation recovery time correlates with bond reforming time.' Letters to Nature 414: 773-776.

Thormann, E., Mizuno, H., Jansson, K., Hedin, N., Fernandez, M.S., Arias, J.L., Rutland, M.W., Pai, R.K., and Bergström, L. (2012). 'Embedded proteins and sacrificial bonds provide the strong adhesive properties of gastroliths.' Nanoscale 4: 3910-3916.

van Oss, C.J., Chaudbury, M.K., and Good, R.J. (1988). 'Interfacial Lifshitz-van der Waals and polar interactions in macroscopic systems.' Chemical Reviews Vol. 88. No. 6. P. 927-941.

Vrålstad, H., Spets, Ö., Lesaint, C., Lundgaard, L., Sjöblom, J. (2009). 'Dielectric properties of crude oil components.' Energy Fuels 23: 5596-5602.

Vuorinen, M. (1999). 'A new ultrasonic method for measuring stripping resistance of bitumen on aggregate.' Licentiate Thesis, Helsinki University of Technology.

Wallqvist, V., Claesson, P. M., Swering, A., Schoelkopf, J., Gane, P.A.C. (2006). 'Interaction forces between talc and hydrophobic particles probed by AFM.' Colloids and Surfaces A: Physiochemical and Engineering Aspects 277: 183-190.

Wallqvist, V., Claesson, P. M., Swerin, A., Schoelkopf, J., and Gane, P.A.C. (2007). 'Interaction forces between talc and pitch probed by atomic force microscopy.' Langmuir 23(8): 4248-4256.

Wallqvist, V., Claesson, P. M., Swerin, A., Schoelkopf, J., and Gane, P.A.C. (2009A). 'Influence of wetting and dispersing agents on the interaction between talc and hydrophobic particles.' Langmuir 25(12): 6909-6915.

Wallqvist, V., Claesson, P. M., Swerin, A., Östlund, C., Schoelkopf, J., and Gane, P.A.C. (2009B). 'Influence of surface topography on adhesive and long-range capillary forces between hydrophobic surfaces in water.' Langmuir 25(16): 9197-9207.

Web Mineral (2011). [Electronic]. Available: http://webmineral.com/chemical.shtml [2011-03-08].

Wiehe, I. A. (1996). 'Two-dimensonal solubility parametermapping of heavy oils.' Fuel Science and Technology International 14(1, 2): 289-312.

Wikipedia (2014). http://www.wikipedia.org/wiki: Retrieved 2014-2001-2027.

Zenkiewicz, M. (2007). 'Methods for the calculation of surface free energy of solids.' Journal of Achievements in Materials and Manufacturing Engineering 24(1): 137-145.